DISSERTATIONES ASTRONOMIAE UNIVERSITATIS TARTUENSIS
13

DISSERTATIONES ASTRONOMIAE UNIVERSITATIS TARTUENSIS
13

ANNA ARET

Evolutionary separation of mercury isotopes in atmospheres of chemically peculiar stars

TARTU UNIVERSITY
PRESS

This study was carried out at the Tartu Observatory, Estonia.

The Dissertation was admitted on April 30, 2009, in partial fulfilment of the requirements for the degree of Doctor of Philosophy in physics (astrophysics), and allowed for defence by the Council of the Institute of Physics, University of Tartu.

Supervisor: Prof. Arved–Ervin Sapar,
Tartu Observatory,
Estonia

Opponents: Dr. Habil. Gražina Tautvaišienė,
Institute of Theoretical Physics and Astronomy of Vilnius University,
Vilnius, Lithuania

Dr. Jiří Kubát
Astronomical Institute of the Academy of Sciences of the Czech Republic,
Ondřejov, Czech Republic

Defence: June 5, 2009, University of Tartu, Estonia

ISSN 1406–0647
ISBN 978–9949–19–113–0 (trükis)
ISBN 978–9949–19–114–7 (PDF)

Autoriõigus Anna Aret, 2009

Tartu Ülikooli Kirjastus
www.tyk.ee
Tellimus nr. 165

CONTENTS

List of original publications **6**

Introduction **8**

1 Research background and objectives **9**
1.1 Characteristic features of CP stars 9
1.2 Isotopic anomalies in CP stars 13
1.3 Formation of elemental and isotope abundance anomalies 22
1.4 Research objectives 28

2 Equations for elemental and isotope separation **30**
2.1 Main equations for diffusion in stellar plasma 30
2.2 Acceleration due to radiation field 32

3 Model computations **38**
3.1 Evolutionary separation of mercury isotopes 38
3.2 Software package SMART 40
3.3 Input data for LID computations 44

4 Results of model computations **47**
4.1 Accelerations of mercury isotopes 47
4.2 Scenario of evolutionary separation of isotopes 49
4.3 Dependence on effective temperature 54
4.4 Dependence on initial mercury abundance 56
4.5 Role of hyperfine splitting of Hg spectral lines 58
4.6 Mercury in the atmospheres of observed HgMn stars 60

5 Discussion **62**

6 Main results of the thesis **64**

Acknowledgements **65**

References **66**

Summary in Estonian **75**

Attached original publications **77**

2

LIST OF ORIGINAL PUBLICATIONS

This thesis is based on the following publications:

I Aret, A. & Sapar, A. 2002, Light–induced drift for Hg isotopes in chemically peculiar stars, Astronomische Nachrichten, 323, 21

II Sapar, A., Aret, A., & Poolamäe, R. 2005, The role of light-induced drift in diffusion of heavy metals and their isotopes in CP stars: an example of mercury, in: Element Stratification in Stars: 40 Years of Atomic Diffusion, ed. G. Alecian, O. Richard, & S. Vauclair, EAS Publications Series 17, 341–344

III Sapar, A., Aret, A., Sapar, L., & Poolamäe, R. 2008a, Segregation of isotopes of heavy metals due to light-induced drift: results and problems, Contributions of the Astronomical Observatory Skalnaté Pleso, 38, 273

IV Sapar, A., Aret, A., Poolamäe, R., & Sapar, L. 2008b, Formulae for study of light-induced drift diffusion in CP star atmospheres, Contributions of the Astronomical Observatory Skalnaté Pleso, 38, 445

V Aret, A., Sapar, A., Poolamäe, R., & Sapar, L. 2008, SMART – a computer program for modelling stellar atmospheres, in: The Art of Modelling Stars in the 21st Century, eds. L. Deng & K.L. Chan, IAU Symposium 252, 41–42

Other related publications of the dissertant:

VI Sapar, A. & Aret, A. 1995, The formation of chemical peculiarities in stellar atmospheres, Astronomical and Astrophysical Transactions, 7, 1

VII Sapar, A., Aret, A., Sapar, L., & Poolamäe, R. 2007a, The separation of isotopes of chemical elements in the atmospheres of CP stars due to light-induced drift, in: Spectroscopic Methods in Modern Astrophysics, ed. L. Mashonkina & M. Sachkov (Moscow: Janus-K), 220–235 (in Russian)

Author's contribution to the publications

The author of the thesis has

- contributed to the derivation of the main formulae describing light-induced drift in the quiescent atmospheres of chemically peculiar stars;
- contributed to the elaboration and debugging of the model atmosphere software package SMART;
- composed the database of mercury spectral lines, taking into account isotopic and hyperfine spectral line splitting;
- carried out capacious and prolonged computations of evolutionary scenarios of diffusional separation of mercury isotopes using computer code SMART;
- given essential contribution to analysis and explication of computed results;
- contributed to writing the papers.

INTRODUCTION

Chemically peculiar (CP) stars are early type main-sequence stars with distinctly abnormal abundances of several elements. These stars are not rare exceptions, the occurrence frequency of CP stars among B5–F5 type main-sequence stars is about 15–20% (Wolff & Preston 1978; Romanyuk 2007). These hot peculiar stars are divided into 4 main classes: metallic-lined (Am), peculiar A-stars (Ap), mercury-manganese (HgMn) and helium-weak (He-weak) stars (Preston 1974).

According to the general opinion the observed anomalous abundances have been generated in the outer layers of the stars by processes that happened after the star had formed, such as diffusion, accretion, magnetic effects, etc. The bulk composition of the entire star is assumed to be normal, reflecting the composition of its natal interstellar cloud. About 40 years ago Michaud (1970) suggested that mechanism responsible for generation of observed peculiarities is radiative-driven atomic diffusion. Diffusive separation of elements takes place in quiescent atmospheres of CP stars, where gravitational settling competes with expelling radiative force in the absence of hydrodynamical mixing processes (see for review Vauclair & Vauclair 1982).

Mercury abundance anomalies have been studied in HgMn stars ever since Bidelman (1962) identified the λ3984 Å feature as due to Hg II. Overabundance of mercury in atmospheres of HgMn stars has been found to be up to 800,000 times solar (e.g. Dolk et al. 2003). Isotopic composition varies significantly from star to star, ranging from the solar system mixture to nearly pure ^{204}Hg (Proffitt et al. 1999; Woolf & Lambert 1999; Dolk et al. 2003).

Michaud et al. (1974) described several scenarios where diffusion could produce the observed abundance and isotopic anomalies of mercury. However, detailed calculations by Proffitt et al. (1999) showed that overabundance of mercury observed in the HgMn star χ Lupi could not be supported in the atmosphere by radiative driven diffusion alone. Explanation of mercury isotope anomalies also seems to require some additional separation mechanism.

Light-induced drift (LID) was put forward by Atutov & Shalagin (1988) as a possible source of isotopic anomalies observed in CP stars. Estimates made by Nasyrov & Shalagin (1993) support the suggestion that efficiency of LID separation may be essentially larger than the effect of radiation pressure. Elaboration of the theory and calculations of Hg isotope separation caused by LID are the main objectives of the present thesis. Obtained results indicate that the Hg isotopic anomalies observed in HgMn stars can be explained by LID, and that an enhancement of heavy isotopes can be expected in CP stellar atmospheres.

CHAPTER 1
RESEARCH BACKGROUND AND OBJECTIVES

1.1 Characteristic features of CP stars

Spectroscopic anomalies among B and A stars were known since the beginning of the 20th century when Annie Cannon noticed, ordering the stars of the Henry Draper survey, that some stars did not fit to the spectral sequence. She provided lists containing 39 silicon stars and 25 strontium stars (Cannon 1912a,b). Comprehensive reviews of the early history of the studies are given by Bidelman (1967) and Wolff (1983).

The term "chemically peculiar star" was first used in 1930-ies for the group of upper-main sequence stars with anomalous chemical composition, determined by studying the widths and profiles of spectral lines. Since "normal star" is assumed to be a solar-composition star, deviation of stellar abundances from solar values (Fig. 1.2) is the criterion to classify a star as a peculiar. There are also chemically peculiar stars on the horizontal branch and among the white dwarfs, but usually the term "CP stars" is used for those which are on the main sequence. The distribution of CP stars in the Hertzsprung–Russell diagram is illustrated in Fig. 1.1 using data for open clusters from North (1993).

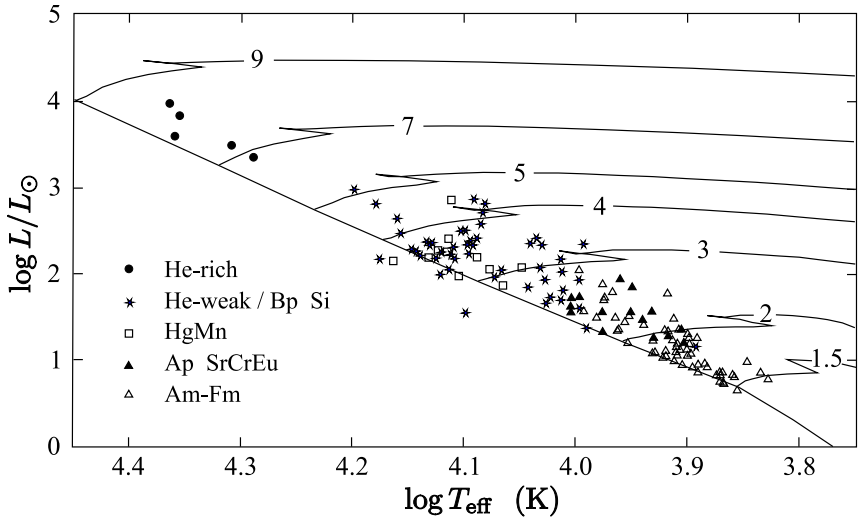

Figure 1.1: The Hertzsprung–Russell diagram for several classes of chemically peculiar stars in open clusters. Evolutionary tracks for solar-composition stars of several initial masses (as indicated) are superposed (Smith 1996a, Fig. 1).

The range of temperatures for atmospheric CP phenomenon is about 7 000 – 20 000 K where the stellar atmospheres are stable: the lower limit corresponds to temperatures where convection is not yet relevant whereas at the upper limit radiatively driven stellar winds start to cause significant mass loss. The distribution of degrees of peculiarity does not show any gap between normal and CP stars (Masana et al. 1998). Even apparently normal A stars show large star-to-star differences in composition (Hill & Landstreet 1993). The difficulty to find a normal A stars as soon as high-quality observations are available suggests that there is a continuous smooth transition from the "normal" to the chemically peculiar stars (Lanz 1993).

The chemically peculiar stars of the upper main sequence were divided by Preston (1974) into four groups according to their peculiar spectral features: CP1 (Am stars), CP2 (classical magnetic Ap stars), CP3 (HgMn stars) and CP4 (He-weak stars).

CP1 Am stars are the coolest of CP stars. Their effective temperature ranges from 7 000 to 10 000 K (spectral classes F5 – A2). These stars are non-variable and do not show any detectable magnetic field. Most of them are in binaries. The heavy metals, beyond the iron peak, are overabundant. Calcium and/or scandium are deficient. The encountered abundance anomalies are usually of 1 to 2 dex at most.

CP2 Magnetic Ap stars are found between 8 000 and 15 000 K of effective temperature (spectral classes F0 – B5). CP2 stars, including both Bp and Ap, possess strong global magnetic fields (Lanz 1993). Overabundances of Si, Cr, Sr, Eu, etc. have been observed. Abundance anomalies are much larger than those of the Am stars and we can often see anomalies of the order of 3 dex with respect to the solar value, and in the most extreme cases even 6 dex. Elements are not evenly distributed over the surface of these stars, they form over- and underabundance spots and rings causing variability of the stars. These spots and rings are believed to be formed due to diffusion in magnetic fields with a large-scale structure. Almost all of CP2 stars have slow rotational velocities.

CP3 HgMn stars are non-magnetic peculiar stars with effective temperature between 10 000 and 15 000 K (spectral classes A2 – B8). They are sometimes considered as an extension towards hotter temperatures of the CP1 group (Wahlgren & Dolk 1998; Adelman et al. 2003). HgMn stars have strong mercury and manganese absorption lines in their spectra. Many other heavy elements are also overabundant. The anomalies are of the same order of magnitude as for the magnetic Ap stars but often not for the same elements (Adelman 1987, 1988, 1989, 1992, 1994; Adelman et al. 2001, 2004, 2006; Smith & Dworetsky 1993; Smith 1993, 1994, 1996b, 1997). Ultraviolet

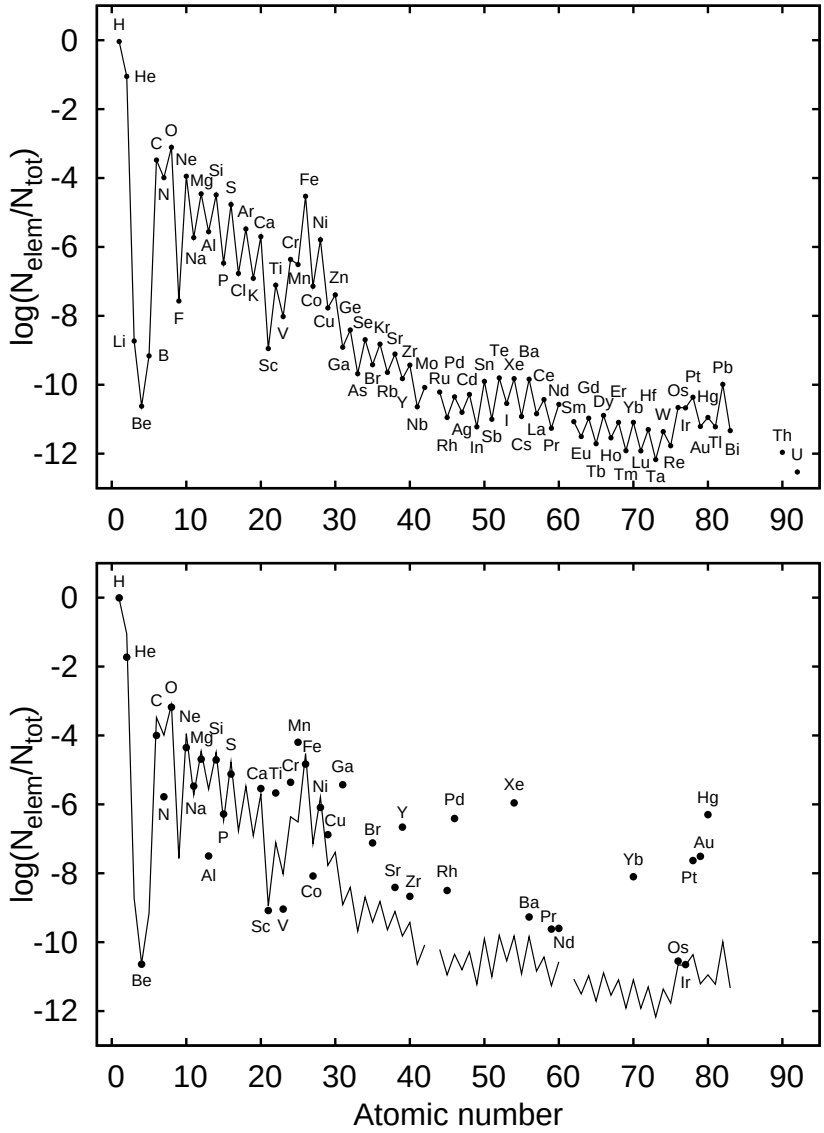

Figure 1.2: Abundances of HgMn star HD 175640 (Castelli & Hubrig 2004a) plotted as dots in the lower panel, compared with solar system abundances (Anders & Grevesse 1989) plotted in the upper panel and shown as solid line in the lower panel.

spectra of unprecedented resolution and photometric quality obtained for HgMn stars χ Lupi, κ Cancri and HR 7775 with Hubble Space Telescope (Wahlgren et al. 1995; Leckrone et al. 1999; Brandt et al. 1999; Proffitt et al. 1999) enabled detailed analysis of abundance and isotopic composition of these stars. Abundances of HgMn star HD 175640 (Castelli & Hubrig 2004a) compared with solar abundances are shown as example in Fig. 1.2. These non-variable stars are also characterised by very slow rotational velocities. According to Wolff & Preston (1978) 70% of slowly rotating ($v \leq 5$ km s^{-1}) late B-type stars are HgMn stars. About half of CP3 stars are found in binaries (Schneider 1986), but it is worth to mention that HgMn stars in binaries do not appear different from single HgMn stars. These stars have not any regular magnetic field. Conti (1969), Borra & Landstreet (1980) and Landstreet (1982) did not find evidence of longitudinal magnetic fields in CP1 and CP3 stars within limits around 100 to 200 G. Only weak magnetic fields have been detected by Mathys & Hubrig (1995), Hubrig & Castelli (2001) and more recently by Hubrig et al. (2006).

CP4 The last group consists of the helium-weak stars. Their effective temperature ranges from 14 000 to 21 000 K. Helium abundance is 1–2 orders of magnitude lower than the solar value. We can distinguish a subgroup with anomalous isotopic ratios between ^{3}He and ^{4}He. While He is globally underabundant, the abundance of lighter isotope ^{3}He is anomalously high. Preston (1974) regrouped the stars with helium peculiarities in the CP4 group, but later on the heterogeneous composition of this group was pointed out. Some CP4 stars are related to the CP3 stars with strong spectral lines of P II, Ga II and Y II, while the other CP4 stars are connected with CP2 stars with strong Si II lines and an observed magnetic field. These CP4 stars are generally hotter (13 000 to 18 000 K) and appear to extend the two sequences of magnetic and non-magnetic CP stars (Lanz 1993).

To complete this picture of the chemically peculiar stars of the upper main sequence, one ought to mention the metal-weak λ Bootis stars and the He-rich early B-stars (Wolff 1983). He-rich stars are the hottest ($T_{\rm eff}$ = 21 000 – 30 000 K) and the most massive CP stars with very strong stellar winds.

Although the groups of CP stars are well-characterized, the boundaries between groups are somewhat blurred. Some stars have properties found in more than one group and there is also a large scatter of abundance patterns among stars assembled in a same group (Takada-Hidai 1991; Lanz 1993). The general properties of CP stars have been described by Preston (1974), Wolff (1983) and in several reviews (e.g. Adelman & Cowley 1986; Cayrel et al. 1991; Takada-Hidai 1991; Ryabchikova 1991; Smith 1996a; Romanyuk 2007).

1.2 Isotopic anomalies in CP stars

Study of isotopic anomalies demands high-resolution observational spectra and precise data on isotopic and hyperfine splitting of spectral lines of a studied element. First isotopic anomaly found from stellar atomic spectra was overabundance of ^{3}He in the atmosphere of the peculiar star 3 Cen A (Sargent & Jugaku 1961). Developments in observational high-precision and high-resolution spectroscopy made possible also studies of isotopic composition of heavy elements in stellar atmospheres. Isotopic anomalies of lithium, mercury, platinum, xenon, thallium and calcium have been found in several CP stars (Cowley et al. 2008).

Helium

Since Sargent & Jugaku (1961) identified ^{3}He in stellar spectra, the presence of ^{3}He anomaly have been reported for several CP stars. The most complete study was carried out by Hartoog & Cowley (1979). They examined a sample of He-weak, normal, and hot peculiar stars and listed 8 stars where the presence of ^{3}He was definite, and another three probable cases. Zakharova & Ryabchikova (1996) studied ^{3}He isotopes in the atmospheres of HgMn stars. Heber (1991) discussed the behaviour of ^{3}He in a number of horizontal branch stars. Most of the ^{3}He stars show a mixture with ^{4}He, some have nearly pure ^{3}He. All of the ^{3}He-enhanced stars simultaneously exhibit a general helium deficiency in their atmospheres (Zakharova & Ryabchikova 1996). Bohlender (2005) found evidence of He isotopic separation in the atmospheres of hot PGa stars 3 Cen A and HR 7467. He showed that in both stars ^{3}He was concentrated in the layer $-2.5 < \log\tau < -1.50$ while ^{4}He has a tendency to settle down below $\log\tau = -0.5 \ldots -0.2$.

Lithium

For the most stars, the ratio ^{6}Li/^{7}Li is below 0.10 (Herbig 1965). Abnormal isotope ratio ^{6}Li/^{7}Li = 0.2 – 0.5 has been found by Polosukhina and her colleagues in several slowly rotating CP stars during international project "Lithium in magnetic CP stars" which started in 1996 (Polosukhina et al. 2004; Polosukhina & Shavrina 2007). Their results also indicate vertical stratification of lithium in the atmospheres of CP stars with an anomalous isotopic composition.

Mercury

Mercury has seven stable isotopes: five even-A isotopes ^{196}Hg, ^{198}Hg, ^{200}Hg, ^{202}Hg, ^{204}Hg, and two odd-A isotopes ^{199}Hg and ^{201}Hg (Table 1.1). The abundance of mercury and it's isotopes has been studied for HgMn stars from optical (e.g., Cowley & Aikman 1975; White et al. 1976; Heacox 1979; Smith 1997; Woolf & Lambert 1999; Dolk et al. 2003) and ultraviolet (Leckrone 1984; Smith 1997; Proffitt et al. 1999) spectra. The most extensive studies of isotopic

structure have been undertaken by Woolf & Lambert (1999) who determined Hg abundances for 42 HgMn stars and isotopic mixtures for 20 stars, and more recently by Dolk et al. (2003) who derived Hg isotopic abundances for 30 HgMn stars. Atmospheric overabundance of mercury in many HgMn stars is extreme, up to solar + 5.9 dex (Dolk et al. 2003). The highest mercury excess of any CP star (solar + 6.27 dex) has been reported for HD 65949 by Cowley et al. (2006), but it is not a mercury-manganese star. Isotopic abundances of mercury range from the solar system (terrestrial) mixture to virtually pure ^{204}Hg (Table 1.1). Above-mentioned studies also reveal that heavier mercury isotopes tend to dominate in cooler HgMn stars, while the hotter HgMn stars have isotopic pattern close to the terrestrial mixture.

Probably the most studied mercury spectral line is λ3984 Å line of Hg II ($6s^2\ ^2D_{5/2} \rightarrow 6s6p\ ^2P_{3/2}$). This line is well observable with both ground-based and space-based instruments, and it has also a very large isotope shifts. These large shifts are caused by nuclear volume effects. Observed profiles of λ3984 Å line for several HgMn stars are shown in Figs. 1.3 and 1.4.

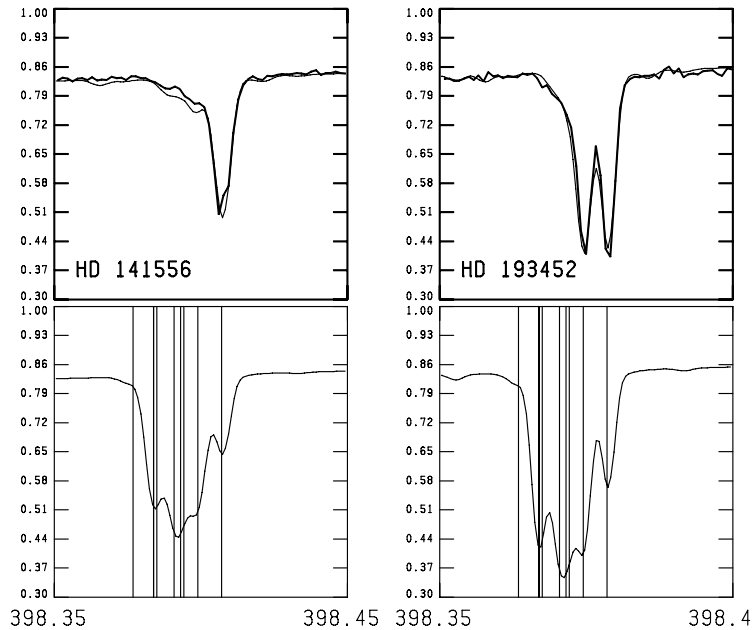

Figure 1.3: Observed spectra (thick lines) of stars χ Lupi and HR 7775 plotted with the best-fit synthetic isotope mixture (thin lines). For both stars the expected profile for the same Hg overabundance, but for terrestrial isotopic composition is shown in the lower panels. The vertical lines indicate the wavelengths of the different isotopic and hyperfine components (Hubrig et al. 1999, Fig. 1).

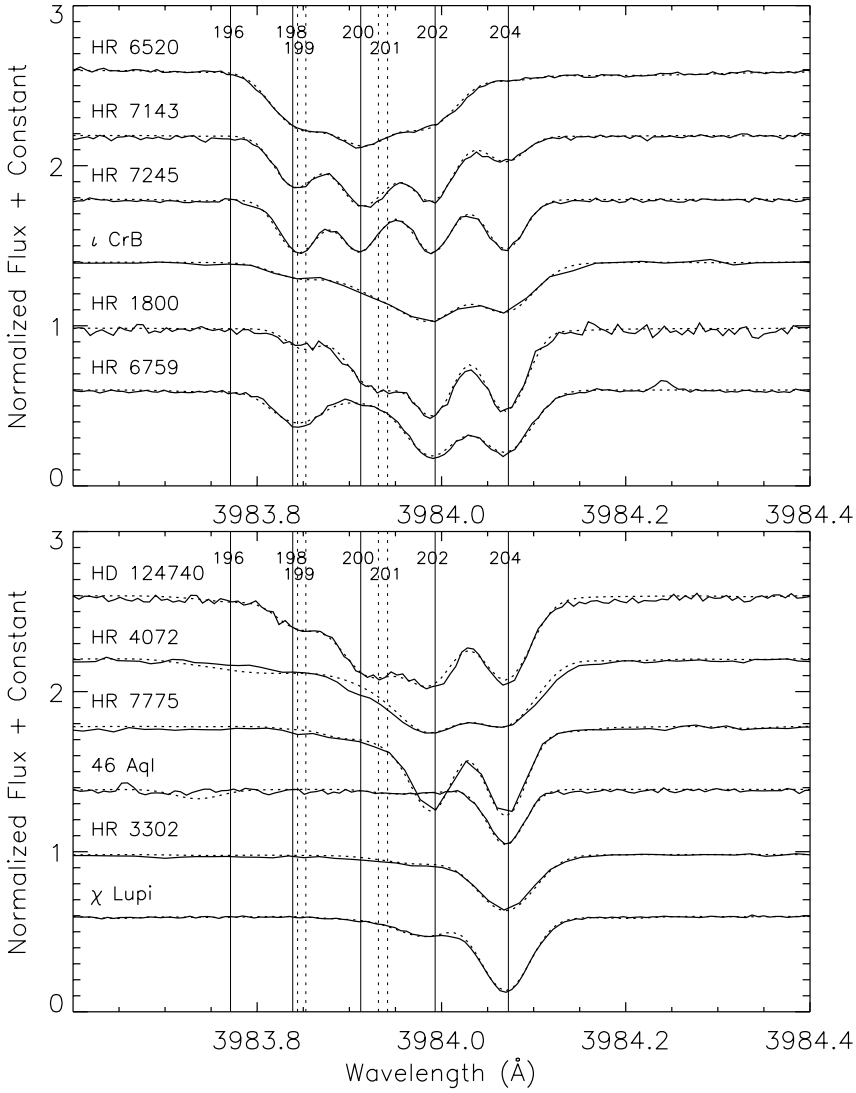

Figure 1.4: Observed spectra of sharp-lined HgMn stars plotted with the best-fit synthetic isotope mixture. The stars are ordered by the relative strength of the ^{204}Hg feature. The solid and dotted vertical lines indicate the wavelengths for the isotope and hyperfine components, respectively (Dolk et al. 2003, Fig. 2).

Table 1.1: Abundance and isotope mixture of mercury derived by Dolk et al. (2003) for HgMn stars. Isotope mixture has been determined from Hg II λ3984 Å line. Mercury abundance $\log N_{\rm Hg}$ is given on a scale where $\log N_{\rm H}$ = 12.00.

Star	$T_{\rm eff}$, K	$\log N_{\rm Hg}$	Isotope mixture, %						
			196	198	199	200	201	202	204
Terrestrial[a]		1.13	0.15	9.97	16.87	23.10	13.18	29.86	6.87
HD 124740	10 350	6.40	0.0 ± 0.2	0.75 ± 0.3	0.75 ± 0.3	7.0 ± 1.0	4.0 ± 0.5	43.0 ± 4.0	44.5 ± 4.0
ν Cnc	10 375	4.95	0.0 ± 0.5	0.0 ± 0.5	0.1 ± 0.5	0.5 ± 1.0	0.7 ± 1.0	35.0 ± 10.0	63.7 ± 15.0
χ Lupi	10 608	6.40	0.0 ± 0.1	0.0 ± 0.1	0.0 ± 0.1	0.0 ± 0.1	0.1 ± 0.1	0.7 ± 0.2	99.2 ± 0.3
ϕ Phe	10 612	4.95	0.0 ± 0.3	1.0 ± 0.7	1.0 ± 0.7	1.0 ± 0.5	1.0 ± 0.5	2.0 ± 0.8	94.0 ± 5.0
HR 7775	10 750	6.35	0.0 ± 0.1	0.1 ± 0.1	0.0 ± 0.1	0.0 ± 0.1	0.4 ± 0.2	37.5 ± 2.0	62.0 ± 3.0
HR 4072	10 900	6.70	0.0 ± 0.1	0.0 ± 0.1	0.1 ± 0.1	0.5 ± 0.3	0.7 ± 0.4	45.0 ± 5.0	53.7 ± 5.0
28 Her	10 908	5.35	0.0 ± 0.2	0.5 ± 0.4	0.5 ± 0.4	0.5 ± 0.2	0.5 ± 0.4	2.0 ± 0.8	96.0 ± 3.0
HR 4487	11 020	6.50	0.0 ± 0.5	0.0 ± 1.0	0.0 ± 1.0	70.0 ± 20.0	10.0 ± 8.0	10.0 ± 5.0	10.0 ± 5.0
HR 1800	11 088	6.65	0.0 ± 0.1	0.0 ± 0.2	0.5 ± 0.2	1.5 ± 0.5	3.0 ± 1.5	58.5 ± 4.0	36.5 ± 3.0
ι CrB	11 250	6.10	0.0 ± 0.1	0.8 ± 0.7	0.8 ± 0.6	1.5 ± 1.0	2.5 ± 1.2	58.4 ± 9.0	36.0 ± 5.0
ϕ Her	11 781	5.65	0.0 ± 0.3	3.5 ± 2.0	2.5 ± 1.5	4.0 ± 2.0	2.0 ± 3.0	31.5 ± 10.0	56.5 ± 8.0
56 Aqr	11 977	5.25	0.15 ± 0.2	10.0 ± 10.0	16.9 ± 15.0	23.1 ± 15.0	13.2 ± 20.0	29.8 ± 10.0	6.85 ± 10.0
HR 3302	12 010	5.65	0.1 ± 0.1	0.1 ± 0.2	0.1 ± 0.2	0.1 ± 0.1	0.1 ± 0.3	1.5 ± 0.3	98.0 ± 1.5
υ Her	12 013	6.40	0.0 ± 0.2	1.0 ± 1.0	1.5 ± 1.0	5.0 ± 2.0	0.5 ± 1.0	45.0 ± 11.0	47.0 ± 7.0
HR 7143	12 077	5.65	0.0 ± 0.1	14.0 ± 3.0	5.0 ± 2.0	34.0 ± 1.5	8.0 ± 2.0	33.0 ± 1.5	6.0 ± 0.5
HR 7245	12 193	5.35	0.0 ± 0.1	13.5 ± 4.0	12.0 ± 3.5	24.0 ± 1.0	1.5 ± 0.5	26.0 ± 1.5	23.0 ± 1.0
41 Eri B	12 250	5.75	0.0 ± 0.4	5.0 ± 5.0	5.0 ± 5.0	10.0 ± 7.0	5.0 ± 8.0	47.0 ± 18.0	28.0 ± 10.0
AV Scl	12 400	7.00	0.0 ± 0.3	0.0 ± 0.5	0.8 ± 1.0	2.0 ± 1.5	2.0 ± 2.0	5.0 ± 3.0	90.2 ± 10.0
β Scl	12 476	6.60	0.0 ± 0.5	2.0 ± 5.0	2.0 ± 5.0	4.0 ± 5.0	4.0 ± 8.0	10.0 ± 5.0	78.0 ± 20.0
41 Eri A	12 750	5.50	0.0 ± 0.2	0.0 ± 0.3	0.0 ± 0.3	0.0 ± 0.5	0.0 ± 0.5	3.0 ± 5.0	97.0 ± 5.0
μ Lep	12 750	6.00	0.0 ± 0.4	1.0 ± 2.0	6.0 ± 5.0	12.0 ± 6.0	15.0 ± 10.0	62.0 ± 15.0	4.0 ± 10.0
46 Aql	12 914	4.95	0.0 ± 0.1	0.0 ± 0.1	0.0 ± 0.1	0.0 ± 0.2	1.5 ± 0.4	2.5 ± 0.2	97.0 ± 1.5

87 Psc	13 126	5.75	0.0 ± 0.5	6.0 ± 10.0	12.0 ± 15.0	25.0 ± 15.0	10.0 ± 10.0	37.0 ± 20.0	10.0 ± 15.0
HR 6520	13 163	6.20	0.0 ± 0.1	10.0 ± 4.0	8.0 ± 3.0	58.5 ± 7.0	5.0 ± 2.5	18.0 ± 3.0	0.5 ± 0.3
112 Her	13 294	6.10	0.0 ± 0.2	1.5 ± 1.0	1.5 ± 1.0	3.0 ± 1.5	3.0 ± 2.5	58.0 ± 12.0	33.0 ± 6.0
κ Cnc	13 470	5.80	0.0 ± 0.3	10.0 ± 6.0	10.0 ± 6.0	4.0 ± 6.0	30.0 ± 12.0	30.0 ± 10.0	16.0 ± 5.0
HR 7361	13 570	5.50	0.15 ± 0.3	10.0 ± 6.0	16.9 ± 8.0	23.1 ± 10.0	13.2 ± 7.0	29.8 ± 12.0	6.85 ± 5.0
HR 6759	13 890	6.00	0.0 ± 0.1	2.5 ± 2.0	4.0 ± 3.0	0.5 ± 0.2	0.5 ± 0.3	50.5 ± 10.0	42.0 ± 6.0
θ Hyi	14 106	5.80	0.15 ± 0.5	10.0 ± 10.0	16.9 ± 20.0	23.1 ± 25.0	13.2 ± 15.0	29.8 ± 25.0	6.85 ± 10.0
HR 4089	15 126	5.15	0.0 ± 0.5	0.0 ± 0.5	0.0 ± 1.0	4.0 ± 5.0	8.0 ± 5.0	43.0 ± 15.0	45.0 ± 10.0

[a] Terrestrial isotope mixture: Rosman & Taylor (1998); solar system (meteoritic) abundance: Asplund et al. (2005).

Table 1.2: Abundance and isotope mixture of platinum derived by Hubrig et al. (1999) for HgMn stars. Platinum abundance $\log N_{\rm Pt}$ is given on a scale where $\log N_{\rm H}$ = 12.00.

Star	$T_{\rm eff}$, K	$\log N_{\rm Pt}$	Isotope mixture, %					
			190	192	194	195	196	198
Terrestrial[a]		1.64	0.01	0.78	32.97	33.83	25.24	7.16
χ Lupi	10 608	5.64	—	—	0.00	0.00	10.00	90.00
HR 7775	10 750	6.23	—	—	0.00	17.50	55.00	27.50
HR 1800	11 088	5.04	—	—	0.00	0.00	0.00	100.00

[a] Terrestrial isotope mixture: Rosman & Taylor (1998); solar system (meteoritic) abundance: Asplund et al. (2005).

Platinum

Isotopic variations of platinum were first determined by Dworetsky & Vaughan (1973) studying Pt II line λ4046 Å in spectra of HgMn stars. Kalus et al. (1998) derived platinum isotope mixture in stars χ Lupi and HR 7775 from high-resolution ultraviolet spectra obtained with Hubble Space Telescope. Abundances of the individual isotopes in HR 7775 have been also determined from optical spectra by Bohlender et al. (1998) and Wahlgren et al. (2000). Hubrig et al. (1999) derived platinum isotopic abundances for three stars – HR 1800, χ Lupi and HR 7775 – from high-resolution spectra obtained at the European Southern Observatory. These stars are overabundant in platinum 3.40 dex, 4.00 dex and 4.59 dex correspondingly, compared to the solar value. These studies show that the isotopic mixtures are dominated by the two heaviest stable isotopes – ^{196}Pt and ^{198}Pt (Table 1.2).

Calcium

The "newest" isotopic anomaly being extensively investigated during recent years is calcium isotopic anomaly. For the first time observational evidence for an anomalous isotopic structure of Ca II in HgMn stars was presented by Castelli & Hubrig (2004b). They reported that Ca II infrared triplet lines in a number of stars showed significant redshifts indicating presence of heavy calcium ^{48}Ca. In extreme case of star HD 175640 (HR 7143) only the heaviest isotope ^{48}Ca was found in the atmosphere. This is a very striking result as ^{48}Ca makes up only 0.187% of the terrestrial calcium mixture. Cowley & Hubrig (2005) found similar anomalies in magnetic CP stars. Cowley et al. (2007) studied shifts of infrared triplet lines of Ca II in the spectra of nearly 70 HgMn and magnetic Ap stars. They concluded that the observed λ8542 shifts are consistent with an interpretation in terms of ^{48}Ca. Ryabchikova et al. (2007, 2008) performed accurate analysis of the Ca isotopic composition and stratification in the atmospheres of 23 magnetic chemically peculiar (Ap) stars. They found that Ca was strongly stratified in 22 out of 23 studied stars (Fig. 1.5), being usually overabundant in deep layers of atmosphere and strongly depleted above $\log \tau_{5000} = -1.5$. They also concluded that observed spectral line features may be explained if the heavy isotope is pushed to the highest atmospheric layers, while the deepest layers may have a nearly solar mixture – primarily ^{40}Ca (Fig. 1.6). This vertical isotopic separation disappears in stars with magnetic field strength above 6–7 kG. Ryabchikova et al. (2008) suggested that observed Ca stratification and isotopic separation may be explained by a combined action of the radiatively-driven diffusion and the light-induced drift.

Investigation completed by Cowley et al. (2009) confirmed that the profiles of strong lines in CP stars cannot be fitted by classical models with homoge-

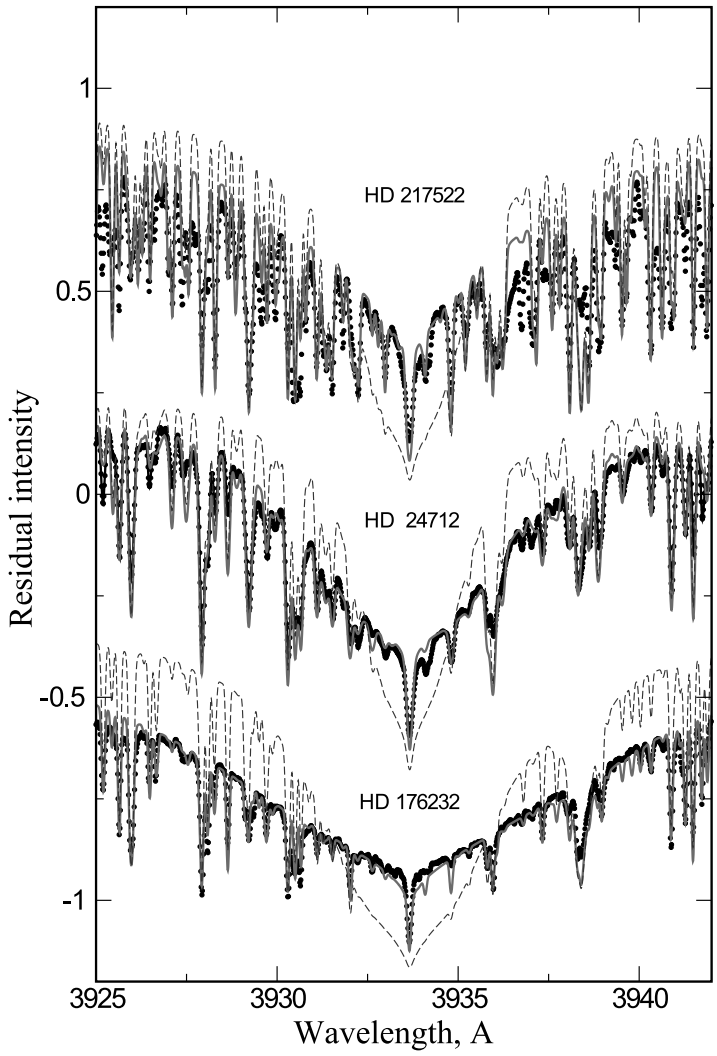

Figure 1.5: Comparison between the observed profiles (symbols) of the Ca II λ3933 Å line and calculations with the stratified (solid line) and homogeneous (dashed line) Ca distributions for 3 stars. The spectra of HD 24712 and HD 176232 are shifted downwards for display purpose (Ryabchikova et al. 2008, Fig. 3). Cores and wings of observed Ca lines cannot be simultaneously fitted by synthetic spectra calculated with homogeneous Ca distribution, while profiles calculated with stratified Ca give a good agreement with observations.

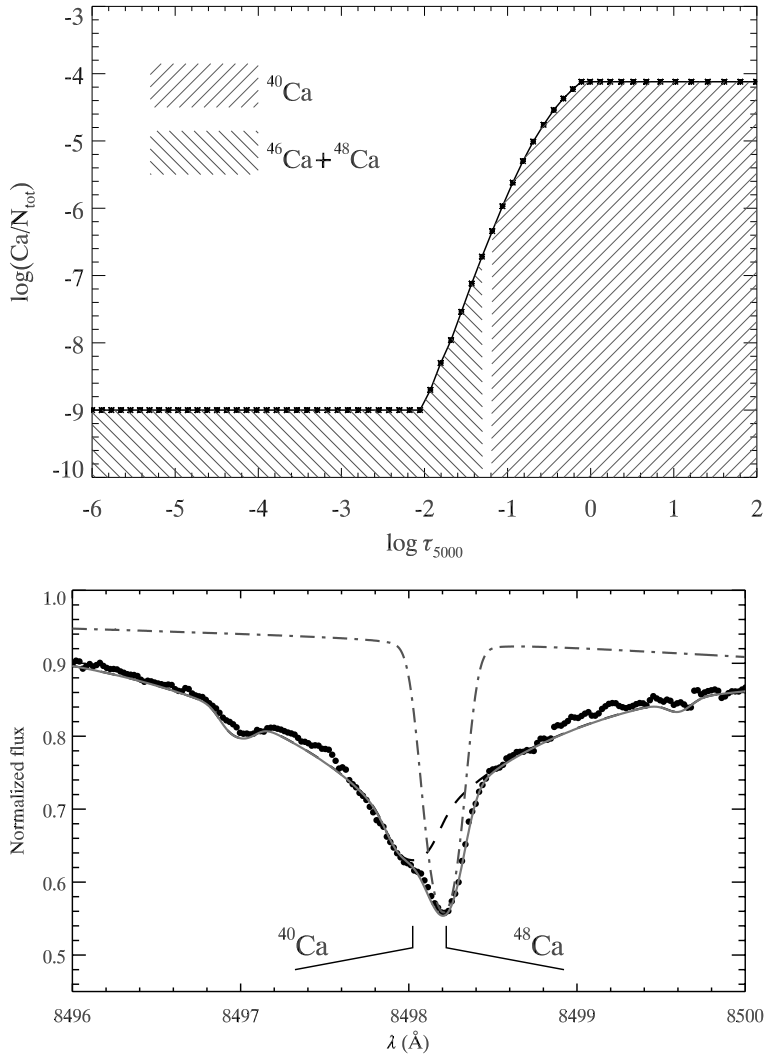

Figure 1.6: Top panel: vertical stratification and isotopic separation of Ca derived by Ryabchikova et al. (2008) for 10 Aql (HD 176232). The overall Ca abundance profile is shown with the solid line. The hatched areas demonstrate vertical separation of Ca isotopes.
Bottom panel: observed Ca II λ8498 Å line profile (symbols) and synthetic profile (solid line) calculated with the stratified Ca distribution. ^{40}Ca and ^{48}Ca contributions are shown by dashed and dashed-dotted lines, respectively (Ryabchikova 2008, Fig. 6).

neous vertical abundance distribution of elements. They also support the claim of Ryabchikova et al. (2008) that the calcium isotopes have distinct stratification profiles for the stars 10 Aql, HR 1217, and HD 122970, with the heavy isotope concentrated toward the higher layers.

Other elements

Other elements for which isotopic composition has been studied include *xenon* (Castelli & Hubrig 2007), *thallium* (Leckrone et al. 1996; Johansson et al. 1996) and *osmium* (Wahlgren et al. 1998). Analysing spectra of Xe-rich peculiar stars HR 6000, 46 Aql and Feige 86 Castelli & Hubrig (2007) noticed that several Xe II lines seemed to be shifted by about -0.1 Å from the predicted position, while most of the lines lied at the laboratory wavelength. They suggested that the wavelength shift could be due to some isotopic anomaly. Unfortunately, lack of atomic data restricts study of xenon isotopic structure in the spectra of the CP stars. Studies of the ultraviolet spectra of HgMn star χ Lupi obtained with the Hubble Space Telescope Goddard High Resolution Spectrograph (HST/GHRS) revealed the other two isotopic anomalies. Presence of heavy osmium isotope ^{192}Os was reported by Wahlgren et al. (1998). Os II lines in the spectrum appeared as a blend of two most-abundant isotopic components with the majority of the heaviest one, ^{192}Os. The large overabundance of thallium (solar + 3.8 dex) and presence of only the heaviest isotope ^{205}Tl was detected by Leckrone et al. (1996).

Regularities of observed isotopic anomalies

Isotopic anomalies of several elements are observed in many HgMn stars. Probably most extreme anomalies are found in cool HgMn star χ Lupi, where Hg (White et al. 1976; Proffitt et al. 1999), Pt (Kalus et al. 1998) and Tl (Leckrone et al. 1996) are dominated by the heaviest isotope. All these elements are overabundant relative to solar system abundances by $4-5$ dex. Proffitt et al. (1999) also point out that dramatically different abundances are derived from lines of different ionization states. Since this ionization anomaly cannot be explained as a non-LTE effect, it may be caused by strong vertical stratification of these elements. Direct observational evidence of such stratification is found for calcium.

Studies of stars with anomalies of light elements such as He and Li show overabundance of lighter isotopes. Indications of isotopic separation also have been found. In the case of light elements the lighter isotope lies in the upper atmospheric layers above the heavier isotope.

Although the overall picture of isotope variations is complex, there is a general trend for heavy elements to show overabundance of heavier isotopes and for light elements – overabundance of lighter isotopes in upper layers of stellar atmosphere. Such trend is consistent with regularities of isotope separation due to light–induced drift (see Section 2.2.2).

1.3 Formation of elemental and isotope abundance anomalies

Since the first observations of abundance anomalies in the CP stars, several hypotheses have been proposed to explain these anomalies. At first they were interpreted in terms of nuclear reactions (Fowler et al. 1965). Interior nucleosynthesis in a post-main-sequence phase of evolution could not, however, reproduce the details of the observations, which became more and more precise. Several mechanisms of surface contamination of a normal star by a supernova companion (Guthrie 1967) or by selective magnetic accretion of interstellar matter (Havnes & Conti 1971) were also discussed, but did not lead to a successful theory.

The importance of the stratification of chemical elements inside stars due to atomic diffusion was pointed out by Sir Arthur Eddington already in the beginning of the 20th century (Eddington 1926). He predicted presence of chemical differences between stars, which were not observed at that time. Early attempts to involve atomic diffusion in order to explain the observations failed (see for review Vauclair & Vauclair 1982; Praderie 2005).

Breakthrough paper of Michaud (1970) ushered in a new era. Selective radiation pressure was included in a diffusion equation as a force able to support elements in stars and form abnormal abundance patterns. The number of papers on the subject of diffusion increased drastically after 1970 (Preston 2005). At the present time almost nobody doubts, that atomic diffusion is responsible for a large part of the abundance variations observed in stars.

Radiative-driven diffusion was at first applied to Ap stars, field of application soon expanded to the Am stars, and then to B-type subdwarfs, white dwarfs and horizontal branch stars. Diffusive gravitational settling plays now a central role in explanation of observed lithium abundances. Recently developed helio- and asteroseismology are new tools which help to test atomic diffusion in several ways (e. g. Vauclair 2005; Turcotte & Richard 2005; Kurtz et al. 2007).

1.3.1 Diffusion theory

The microscopic diffusion is a physical process resulting from random motion of particles which generates a flow of matter due to a density gradient, a temperature gradient and an external force. The diffusion velocities are in the most cases very slow. Therefore, the microscopic diffusion can only have significant effects in very stable media. On the main sequence, this condition is fulfilled in atmospheres of stars with $T_{\rm eff}$ between approximately 7 000 and 20 000 K.

Michaud (1970) suggested, that abundance anomalies observed in Ap stars were generated by diffusion processes driven by competing gravitational and radiative forces. Review of the theory and early studies is given by Vauclair & Vauclair (1982).

Main statements of diffusion theory:

- anomalous abundances form in atmosphere of a star, the bulk composition of entire star is normal;
- abundance anomalies in CP stars are generated by atomic diffusion;
- stratification of elements and their isotopes is mainly determined by interplay between gravitational and radiative forces;
- particle diffusion only works in quiescent atmospheres, where convection and turbulence, mass loss by stellar wind and meridional circulation are weak enough;
- diffusion time scales and equilibrium abundances are strongly affected by competing macroscopic motions;
- in magnetic stars diffusion is strongly affected by magnetic field.

Main expressions for diffusion of chemical elements in stellar atmospheres are given in Chapter 2.

Already early studies (Michaud et al. 1976; Cowley & Day 1976) showed, that when radiative acceleration was included, atomic diffusion could explain the observed abundance anomalies in the stellar envelopes. However, the expected anomalies are generally much larger than those observed in individual stars, suggesting that some competing hydrodynamical processes reduce the effects of atomic diffusion. The most favoured competing processes are mass loss (Michaud et al. 1983) and turbulence (Vauclair et al. 1978).

Evolutionary stellar models with radiative-driven diffusion have been constructed by Michaud and his colleagues for AmFm stars (Richer et al. 2000; Michaud et al. 2005), Population II stars (Richard et al. 2002b,a; VandenBerg et al. 2002) and horizontal branch (HB) stars (Michaud et al. 2007, 2008). HB stars are very closely related to HgMn stars (Michaud & Richer 2008). These models do not include detailed atmospheric modelling and assume chemically homogeneous mixed outer region. Radiative accelerations have been found using so-called "diffusion approximation" for photon flux (Milne 1927). This approximation is valid in optically thick medium of stellar interiors where $\tau \gg 1$. The concentration variations within HB and AmFm stars obtained by evolutionary computations are illustrated in Fig. 1.7.

Stellar evolution models have been relatively successful at explaining peculiarities of AmFm stars. However, not all abundance anomalies of HgMn and HB stars can be reproduced. Isotopic anomalies observed in HgMn stars also remained unexplained. Michaud & Richer (2008) suggested that there is additional

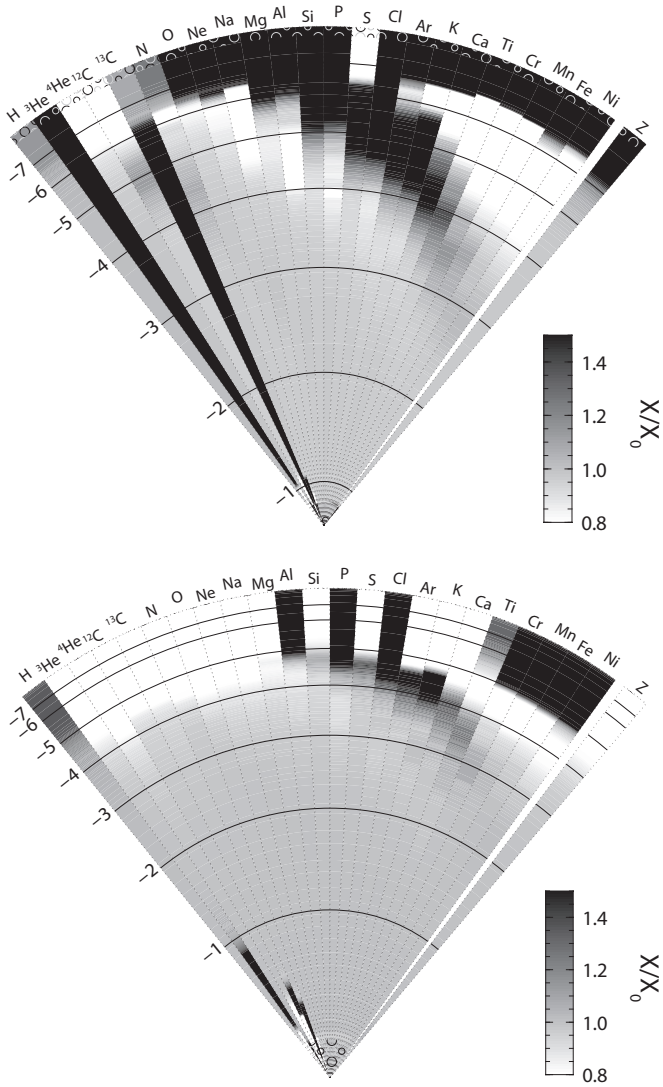

Figure 1.7: Concentration variations in a HB star model (top panel) with $M_* = 0.61 M_\odot$ and $T_{\rm eff} \sim 12400\,$K after 30 Myr on the HB and in AmFm (Pop I) star model (bottom panel) with $M_* = 2.0 M_\odot$ and $T_{\rm eff} \sim 8000\,$K after 616 Myr on the main sequence. The radial scale is linear in r, labels at arcs show logarithm of mass fraction above certain radius, $\log(\Delta m/M_*)$. The outer 50% by radius is affected by diffusion in the HB model while it is the outer 25 % by radius in the Pop I model (Michaud & Richer 2008, Fig. 1).

separation going on in the atmospheric regions. They write: "The presence of isotope anomalies is probably the strongest argument in favour of separation going on in the atmosphere in addition to the bottom of the mixed zone, both in HgMn stars and the probably related HB stars". This suggestion is strongly supported also by observational evidence of stratification of chemical elements in stellar atmospheres accumulated during recent years. I have already discussed in Section 1.2 stratification of He (Bohlender 2005), Li (Polosukhina & Shavrina 2007) and Ca (Ryabchikova et al. 2008; Cowley et al. 2009) observed in atmospheres of several CP stars. Stratification of N, S, Fe and other metals in HB stars have been detected by Khalack et al. (2007, 2008). Signatures of stratification of Cr (Savanov & Hubrig 2003) and Mn (Thiam et al. 2008) have been found in HgMn stars.

The diffusion process is essentially more difficult to model in a stellar atmosphere than in a stellar interior because the medium is optically thin and "diffusion approximation" cannot be used to obtain photon flux. The radiative transfer equation has to be solved in detail at a large number of frequency points.

Several model atmospheres with equilibrium stratification of elements (diffusion velocities $v_i \approx 0$) and invariable radiative accelerations have been constructed. First such atmospheres were computed for white dwarfs by Werner & Dreizler (1999). Based on the stellar atmosphere code PHOENIX (Hauschildt et al. 1997; Baron & Hauschildt 1998; Hauschildt et al. 1999; Hauschildt & Baron 1999) stratified model atmospheres were computed for blue horizontal branch (BHB) stars (Hui-Bon-Hoa et al. 2000) and Ap stars (Leblanc & Monin 2004). Further development of this atmospheric code is described by Leblanc et al. (2009). Alecian & Stift (2007, 2008) have studied stratification in the atmospheres of magnetic Ap stars. Shulyak et al. (2004) have constructed model atmospheres that empirically include stratification of the elements, recent version of this code incorporates also effects of magnetic field (Shulyak et al. 2008).

All these model atmospheres are constructed without taking into account time-dependent diffusion such as in the evolutionary models. Obtained abundances indicate maximum values that can be supported in the atmosphere by radiation field. However, the formation of abundance anomalies by diffusion is a non-linear process and one cannot be sure that a time-dependent diffusion will lead to a stationary solution (see a comment by G. Alecian to Cowley & Bord 2004).

Diffusion time scales are much smaller in stellar atmospheres than in stellar interiors, also time scales in upper and deep layers of atmospheres differ by several orders of magnitude. These time scales are also strongly affected by competing transport processes like convection, turbulence, meridional flows, mass loss, and by the presence of magnetic fields. Time-dependent calculations require a large

number of time steps and therefore an enormous amount of CPU time. Leblanc et al. (2009) admit, that time-dependent diffusion calculations with huge model atmosphere code PHOENIX running on supercomputers are "not numerically feasible for the moment". PHOENIX is probably the most comprehensive existing model atmosphere code. The detailed modelling of physical processes in stellar atmospheres requires huge computer power. However, simpler atmospheric code which does not take into account so many physical processes in so detailed approximations, could run in the regime necessary for time-dependent diffusion modelling. Model atmosphere code SMART (Sapar & Poolamäe 2003; Aret et al. 2008) is a compact code which enables to carry out evolutionary calculations of diffusive separation of elements and their isotopes in atmospheres of hot stars (Chapter 3).

1.3.2 Diffusion of Hg in atmospheres of HgMn stars

Physical conditions in the atmospheres of HgMn stars are probably the closest approach to the ideal situation of pure diffusion (Vauclair & Vauclair 1982). Macroscopic motions mixing the stellar plasma are weak. These hot stars have no outer convective zone and stellar wind is very weak. Rotation velocities are low, that means meridional circulation also cannot mix the atmosphere. Diffusion processes are strongly affected by magnetic fields, but in HgMn stars they are also very weak or lacking. Binarity also does not seem to influence the phenomenon of HgMn stars: the fraction of HgMn stars found in binaries is about the same as fraction found for normal stars (Schneider 1986).

Michaud et al. (1974) proposed theoretical explanation of mercury isotopic anomalies based on the diffusion theory. According to the proposed scenario (Fig. 1.8), strong radiative force on Hg II pushes mercury to the high atmospheric layers where fraction of doubly ionized mercury increases due to very low density or increase of temperature by some other mechanisms. Much smaller radiative force on Hg III leads then to the accumulation of mercury in these layers and formation of a mercury cloud at small optical depths $\tau \sim 10^{-7}$ – 10^{-9}. In this relatively dense mercury cloud the radiative and gravitational forces on mercury approximately cancel, and the small mass difference between the isotopes would lead to their segregation. Lighter isotopes are then wiped out from the atmosphere by weak stellar wind or are hidden in high layers in the form of Hg III. This finely balanced diffusion process cannot, however, explain several observed isotopic patterns (Woolf & Lambert 1999; Dolk et al. 2003).

Two years later White et al. (1976) suggested a mass-dependent fractionation scheme of isotope separation based on isotopic mixtures observed in HgMn stars ι CrB, χ Lup and HR 4072. They introduced dimensionless mix parameter q

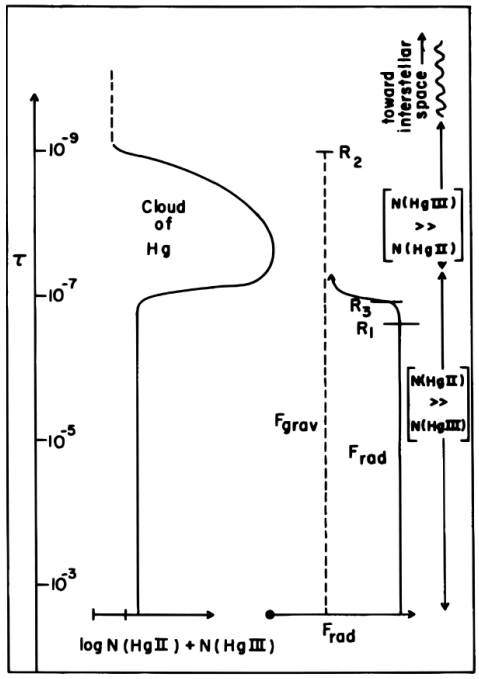

Figure 1.8: Isotope separation scenario sketched by Michaud et al. (1974).

to describe abundances of Hg isotopes relative to ^{202}Hg. This mass-dependent fractionation model was widely used but, as isotopic mixtures were determined for more and more stars, failed to reproduce details of the observations (Jomaron et al. 1998; Hubrig et al. 1999; Proffitt et al. 1999; Woolf & Lambert 1999). For example, isotopic mixtures in HR 7775 and HR 7245 (Table 1.1) cannot be adequately described by the q-parameter.

In the absence of mixing processes the radiative-driven diffusion is the most probable cause of abundance anomalies and element stratification in the atmospheres of HgMn stars. However, this mechanism alone may not account for all observed abundance and isotopic anomalies. Detailed calculations by Proffitt et al. (1999) show that radiative-driven diffusion is unable to support observed large abundance enhancements of mercury in the two HgMn stars χ Lupi and HR 7775. They found that an overabundance by a factor of 10^4 of Hg can be supported by $a_{\rm Hg}^{\rm rad}$ instead of the observed 10^5 overabundance. Similar results were obtained for thallium by Proffitt et al. (1996). Furthermore, there is no simple way of using radiative-driven diffusion mechanism to reproduce versatile isotopic

mixtures of mercury found in HgMn stars (Table 1.1). This suggests that some other physical mechanism(s) are also involved.

Atutov & Shalagin (1988) suggested that effect of light-induced drift (LID), discovered and studied in laboratory experiments (Gel'mukhanov & Shalagin 1979; Popov et al. 1989), may cause isotopic anomalies in CP stars. Nasyrov & Shalagin (1993) presented some numerical estimations of the effect in the conditions similar to those of the atmospheres of CP stars. Light-induced drift appears when radiation flux absorbed by colliding plasma particles is anisotropic within the spectral line widths of an ion. Effect of LID is discussed in Section 2.2.2.

Light-induced drift is particularly effective for separation of isotopes, pushing up isotope with red–shifted spectral lines and sinking isotope with blue–shifted lines. Thus, this effect does not depend on mass of the isotopes, but on the mutual position of their overlapping spectral lines. In the case of light elements like He and Li, spectral lines of the heavier isotope are shifted to shorter wavelengths and therefore LID causes sedimentation of the heavier isotope and levitation of the lighter one. For heavy elements direction of the isotopic shift is opposite (due to nuclear volume effect) and so is the influence of LID. It is very likely that systematic deficiency of lighter mercury isotopes and also the overabundance of lighter isotopes ^{3}He and ^{6}Li observed in many CP stars is caused by LID.

Several other processes may also contribute to the creation of the peculiar abundances in HgMn stars. These include microturbulence, selective stellar winds and entangled magnetic fields. Effects of stellar evolution, stellar rotation and the presence of a binary companion may also influence the development of the observed anomalies. The explanation of HgMn star phenomenon probably lies in a complex interplay between many physical mechanisms and further theoretical studies must be undertaken.

1.4 Research objectives

In spite of numerous attempts, strong isotopic anomalies observed in the atmospheres of chemically peculiar stars have not found acceptable explanation yet. Widely accepted theory of radiative-driven diffusion fails to reproduce the versatility of observed isotope mixtures. Light-induced drift seems to be one of the most probable mechanisms of isotope separation. However, this phenomenon has not been sufficiently studied yet. Probably one of the reasons is that it is difficult to include LID into model computations.

These unsolved problems lead to the main objective of the present thesis: to evaluate phenomenon of light-induced drift as possible mechanism of isotope separation in atmospheres of CP stars.

The first task was to derive formulae for LID in the form suitable for study of separation of isotopes of heavy metals in the CP stellar atmospheres. Adequate approximations had to be found for cross-sections and transition rates of several quantum physical interaction processes involved into LID generation. These formulae could then be used in numerical simulations.

Fast model atmosphere code SMART developed by our working group in Tartu Observatory provided a necessary software basis for modelling the time-dependent diffusive separation of isotopes. Additional code blocks had to be composed to model diffusion processes taking into account both usual radiative acceleration and the light-induced drift.

Mercury has been chosen for numerical simulations since it has most drastic overabundance (up to about 6 dex) in CP atmospheres and isotopic mixtures have been determined for many stars from high-resolution and high signal-to-noise observational spectra. Data for mercury in widely used Kurucz (1993b) spectral line database did not contain isotopic and hyperfine splitting of mercury lines. Therefore necessary database of mercury spectral lines had to be compiled.

Computation of evolutionary scenarios of Hg isotope separation for a set of model atmospheres corresponding to the parameters of HgMn stars was to be carried out to reveal main regularities of the process.

CHAPTER 2
EQUATIONS FOR ELEMENTAL AND ISOTOPE SEPARATION

2.1 Main equations for diffusion in stellar plasma

Time-dependent stratification process in stellar atmospheres is described by two main equations: continuity equation and equation of diffusion velocity. Description of stellar plasma in this thesis is based on the following assumptions:

1. plasma can be considered as dilute gas for which the ideal gas equation of state ($P = NkT$) holds;
2. the Maxwellian velocity distributions and same temperature hold for all ions and electrons;
3. the local thermodynamical equilibrium (LTE) atomic state populations values hold (Boltzmann and Saha equations);
4. diffusion velocities are much smaller than thermal velocities;
5. collisions are dominated by classical interactions between two point particles;
6. magnetic fields are lacking.

Continuity equation for ion j of element i can be written in the form:

$$\frac{\partial \rho_{i,j}}{\partial t} + \nabla(\rho_{i,j} v_{i,j}) = \dot{\rho}_{i,j}, \tag{2.1}$$

where $\rho_{i,j} = m_i N_{i,j}$ is density of ion j with mass m_i, $v_{i,j}$ is diffusion velocity of ion j and $\dot{\rho}_{i,j}$ is the source term due to ionization and recombination. For element i holds $\sum_{j \in i} \dot{\rho}_{i,j} = 0$ and we obtain:

$$\frac{\partial \rho_i}{\partial t} + \nabla(\rho_i v_i) = 0. \tag{2.2}$$

Two formalisms have been commonly used to describe diffusion in stellar plasma, namely the Chapman-Enskog method (Chapman & Cowling 1970) and the Burgers' method (Burgers 1969). A good comparison of these methods can be found in Thoul & Montalbán (2007). Diffusion equation is obtained from approximate solutions of the Boltzmann equation for binary or multiple gas mixtures:

$$\frac{df_i}{dt} \equiv \frac{\partial f_i}{\partial t} + \mathbf{v_i} \cdot \frac{\partial f_i}{\partial \mathbf{r}} + \dot{\mathbf{v}}_\mathbf{i} \cdot \frac{\partial f_i}{\partial \mathbf{v_i}} = Coll(f_i)\ , \tag{2.3}$$

where $f_i = f_i(\mathbf{r}, \mathbf{v}, t)$ is the distribution functions of species i and $Coll(f_i)$ is the binary collision term.

The Chapman-Enskog theory assumes that distribution function of a given species can be found as convergent series. Substituting the disturbed velocity distribution into Boltzmann's equation and carrying out its linearisation one obtains a series of equations for the sequence of approximations. The lowest order approximation is the Maxwellian distribution function.

It has turned out that Burgers' equations are equivalent to the second order approximation of the Chapman-Cowling method (Thoul & Montalbán 2007). Higher-order approximations in the Chapman-Cowling formalism give more accurate results, but they are intractable for multicomponent gases. The Burgers' approach is easier to use in the case of multicomponent gases.

In both methods, the diffusion coefficients can be written as functions of the collision integrals, which depend on the exact nature of the interaction between colliding particles. Whichever of the two methods is used, one of the main difficulties lies in the calculation of the collision integrals (Paquette et al. 1986).

Since the abundance of heavy elements is many orders of magnitude lower than hydrogen abundance, we can neglect interactions between those trace elements and consider every element separately, i.e. stellar plasma can be treated as a combination of binary mixtures.

Diffusion velocity for mixture of two gases can be written as (Chapman & Cowling 1970):

$$v_1 - v_2 = \\ -\frac{N^2}{N_1 N_2} D_{12} \left\{ \nabla \ln \frac{N_1}{N} + \frac{N_1 N_2 (m_2 - m_1)}{N\rho} \nabla \ln P - \frac{\rho_1 \rho_2}{P\rho} (F_1 - F_2) + \frac{D_T}{D_{12}} \nabla \ln T \right\}, \tag{2.4}$$

where v_1, v_2 are the mean velocities of particles 1 and 2, D_{12} is the diffusion coefficient, D_T is the thermal diffusion coefficient, N_1, N_2 are number densities of the two gases (total density $N = N_1 + N_2$), m_1, m_2 are atomic masses of particles 1 and 2, ρ_1, ρ_2 are their mass densities ($\rho_i = m_i N_i$, $\rho = \rho_1 + \rho_2$), P is total gas pressure ($P = P_1 + P_2$), T is temperature and F_1, F_2 represent the external forces on particles 1 and 2 per unit mass (i.e. the accelerations).

In the case of hydrostatic equilibrium $\nabla P = \rho_1 F_1 + \rho_2 F_2$ holds and equation of diffusion velocity reduces to

$$v_1 - v_2 = -\frac{N^2}{N_1 N_2} D_{12} \left\{ \frac{1}{P} \left(\nabla P_1 - \rho_1 F_1 \right) + \frac{D_T}{D_{12}} \nabla \ln T \right\}. \tag{2.5}$$

For a trace element $N_1 \ll N_2$ and the diffusion velocity can be then found as

$$v_1 = -D_{12} \left(\nabla \ln P_1 - \frac{m_1}{kT} F_1 \right) - \frac{N}{N_1} D_T \nabla \ln T \,. \tag{2.6}$$

In stellar atmospheres $\nabla \ln T \ll \nabla \ln P$ and thermal diffusion can be neglected. In this approximation, taking into account that $P = NkT \Rightarrow \nabla \ln P = \nabla \ln N$, we find

$$v_1 = -D_{12}\left(\nabla \ln N_1 - \frac{m_1}{kT}F_1\right). \tag{2.7}$$

Diffusion in non-magnetic stellar atmosphere is mainly determined by competing gravity and radiative acceleration, thus for trace element i in plane-parallel stellar atmosphere the diffusion velocity can be found as

$$v_i = D_i\left(\frac{m_i}{kT}(a_i^{\rm rad} - g) - \frac{d\ln N_i}{dr}\right), \tag{2.8}$$

where g is gravity and $a_i^{\rm rad}$ is acceleration due to radiation.

Equations 2.2 and 2.8 are the main equations to be solved together for modelling diffusional separation of isotopes of chemical elements in stellar atmospheres.

2.2 Acceleration due to radiation field

2.2.1 Usual radiative acceleration

Total acceleration of the element is to be obtained by combining accelerations due to bound-bound and bound-free transitions. Since in atmospheres of CP stars radiative levitation acts primarily through bound-bound atomic transitions, acceleration due to bound-free transitions has been neglected in the present study. Acceleration resulted from bound-bound transition from lower level l to upper level u of ion j can be found as

$$a_j^{\rm ul} = \frac{\pi}{m_j c} X_{j,l} \int_0^\infty \sigma_{ul}^0 V(u,a)\mathcal{F}_\nu d\nu\ , \tag{2.9}$$

where $X_{j,l} = N_{j,l}/N_j$ is state l population fraction, $\pi\mathcal{F}_\nu$ is total monochromatic flux and σ_{ul}^0 is the cross–section of photon absorption in transition $l \to u$, which can be expressed using oscillator strength f_{ul} and Doppler width of spectral line $\Delta\nu_D$ in the form $\sigma_{ul}^0 = \dfrac{\pi\, e^2 f_{ul}}{m_e c \Delta\nu_D}$. Normalized Voigt function due to the thermal Doppler motion and the Lorentz damping is defined by

$$V(u,a) = \frac{a}{\pi^{3/2}} \int\limits_{-\infty}^{\infty} \frac{e^{-y^2}}{(u_\nu - y)^2 + a^2} dy\ . \tag{2.10}$$

The argument of the Voigt function is the dimensionless frequency $u_\nu = \Delta\nu/\Delta\nu_D$, its parameter $a = \gamma/(4\pi\Delta\nu_D)$ is the ratio of characteristic widths

of Lorentz and Doppler profiles. Integration is carried out over the dimensionless velocity $y = v/v_T$, where the thermal velocity $v_T = \sqrt{2kT/m_j}$ and m_j is the mass of the light–absorbing ion.

Additional contribution to the usual radiative acceleration in spectral lines is given by the light-induced drift. Radiative acceleration is almost the same for all isotopes of given element whereas light-induced drift is drastically different for different isotopes and thus can be an effective mechanism of isotope separation.

2.2.2 Light–induced drift

Physics

Atutov & Shalagin (1988) suggested that light-induced drift can be the mechanism causing isotopic anomalies in CP stars. They studied the effect of light-induced drift in laboratory physical experiments (Atutov 1986; Atutov et al. 1986; Popov et al. 1989) as a selective acceleration of atomic particles in spectral lines by monochromatic laser beams. Nasyrov & Shalagin (1993) presented some numerical estimations of the effect in the conditions similar to those of the atmospheres of CP stars.

LeBlanc & Michaud (1993) evaluated LID effect in stars and compared it to the usual radiative accelerations. They found that under optimal conditions ratio $V^{\rm LID}/V^{\rm rad}$ may be up to $2 \cdot 10^2$. Rough estimates of LID effect based on calculation of LID in single spectral line were obtained for helium, lithium, oxygen and mercury. LeBlanc & Michaud (1993) concluded, that LID accelerates the isotopic separation of ^{3}He and ^{4}He, but Li, O and Hg are less affected by LID. They, however, noted that more precise calculations using synthetic spectra including all lines have to be done.

The formulae for computation of LID, which are given in the present thesis were derived by Sapar & Aret (1995) and further improved in several papers (Aret & Sapar 2002; Sapar et al. 2005, 2007a, 2008b). In these papers theory of LID was generalized for the case if, in addition to the Doppler line profile, also the Lorentz damping is taken into account, i.e. for the Voigt profile. Also some additional refinements, which are essential for study of LID in stellar atmospheres, have been made.

The light-induced drift is a result of collisional effects. LID arises when the radiation flux is anisotropic within the spectral line widths of an ion, i.e. the blue or red wing of the line receives a larger radiative flux than the other wing. This causes asymmetry in the excitation rates of atoms and ions with different thermal Doppler shifts. Assume, for example, that the flux in the red wing $\mathcal{F}_R$ is larger than the flux in the blue wing $\mathcal{F}_B$ (Fig. 2.1) of the Doppler broadened spectral line. As a result, there are more excited ions among particles moving downward in the

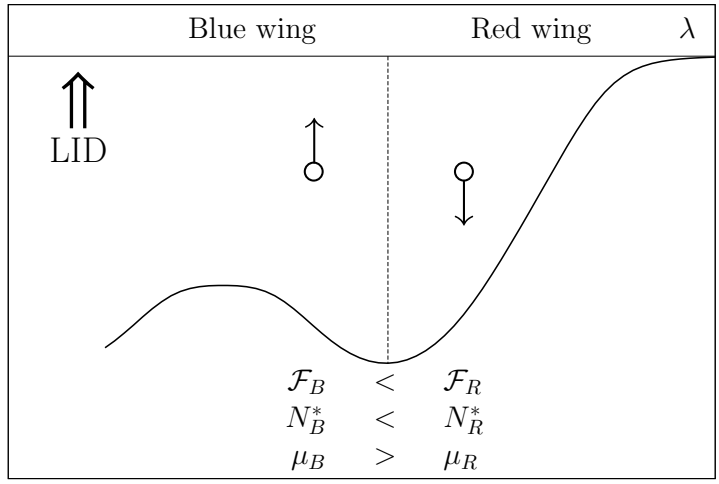

Figure 2.1: Scheme of the LID generation. The arrows show the direction of thermal motion of particles absorbing radiative flux at a given frequency. In the present case particles absorbing radiation in the blue wing of the spectral line receive less flux and have larger mobility giving thus drift in the direction of motion of these particles, i.e. upward.

atmosphere than among moving upward. Since the collision cross-section is larger for atomic particles in the excited (upper) states than in the ground (lower) state, the mean mobility of particles moving upward is larger than the mean mobility of particles moving downward. This imbalance induces a drift velocity upward. Thus, the direction of LID depends on the flux asymmetry in the spectral line: the larger flux in the red wing induces the upward drift, the larger flux in the blue wing – the downward drift.

Usually blending of spectral lines is random and so is the LID direction. Summing over all spectral lines of an element would give a relatively small contribution to radiative acceleration. LID can be important only if the asymmetry of spectral lines is systematic. This is the case for the isotopes. Isotopes with slightly shifted energy levels have overlapping spectral lines, giving systematically similar asymmetry in line profiles. Thus, the LID is most effective for diffusive separation of isotopes.

Isotopic shifts of atomic energy levels are caused by two effects: the mass effect due to the fact that nuclear mass is finite, and the volume effect arising from the distribution of the nuclear charge within a finite volume (Bransden & Joachain 2003). The isotope shift in the atomic spectra of light elements results from the mass effect, nuclear volume effect is negligible. As a result, most spectral lines of

heavier isotopes are blue-shifted relative to the lines of lighter isotope. For heavy elements the volume effect dominates over the mass effect, and consequently isotope shift of spectral lines is the opposite – spectral lines of heavier isotope are shifted to longer wavelengths. Volume effect is most important for low s-states, particularly the ground state.

Consider, for example, a heavy element with only two isotopes (Fig. 2.2).

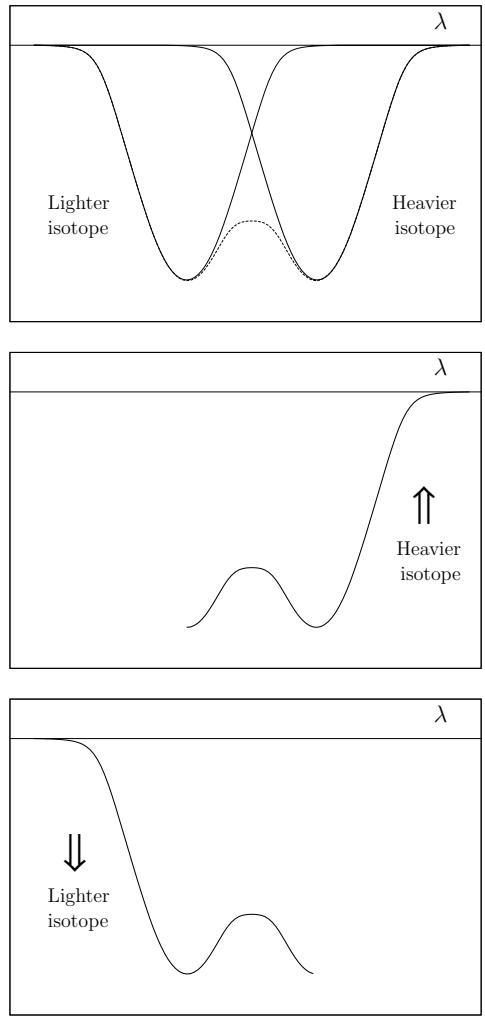

Figure 2.2: Generation of LID due to overlap of isotopic spectral lines of a heavy metal. Heavier isotope with red-shifted spectral line rises and lighter isotope with blue-shifted line sinks.

Due to overlap of isotope spectral lines all lines of the heavier isotope have larger flux in the red wing and all lines of the lighter isotope – in the blue wing. These systematic asymmetries generate LID that causes levitation of the heavier isotope and sedimentation of the lighter one. For light elements (say, for He) the isotope line shift and thus the LID directions are the opposite. Generally, LID causes rising of isotope with red-shifted line and sinking of isotope with blue-shifted line. This means that the overabundance of heavy isotopes of Hg, Pt, Tl etc. and light isotopes of He and Li would be expected. Hyperfine splitting of spectral lines of isotopes with odd number of nucleons is irregular relative to isotopic splitting. This complicates the picture of isotopic separation and can give different results for different chemical elements.

Formulae

LID can be reduced to equivalent acceleration $a^{\rm LID}$ additional to usual radiative acceleration $a^{\rm rad}$ (see attached papers Aret & Sapar 2002; Sapar et al. 2008b). The expression for $a^{\rm LID}$ is similar to the formula for $a^{\rm rad}$ (Eq. 2.9) but instead of Voigt function (Eq. 2.10) there is its derivative relative to the wavelength. Thus, the equivalent acceleration due to LID in transition $l \to u$ of ion j of the element i can be found as

$$a_j^{\rm LID} = \varepsilon q \frac{\pi}{m_i c} \int\limits_0^\infty X_{j,l}\, \sigma_{ul}^0\, \frac{\partial V(u,a)}{\partial u} \mathcal{F}_\nu d\nu \,. \tag{2.11}$$

Coefficient q is the ratio of particle and photon momenta:

$$q = \frac{m_i v_T c}{2h\nu} = \frac{m_i v_T}{2} : \frac{h\nu}{c}$$

and ε is the efficiency of LID given by

$$\varepsilon = \frac{C_u - C_l}{A_u + C_u} \,, \tag{2.12}$$

where C_u and C_l are collision rates for particles in upper and lower state, A_u is the total rate of spontaneous transitions from the upper state. Thus efficiency of LID ε depends on probability that electron stays on the upper level until the next collision.

Collision rates for impacts between ions have been calculated using long-range Coulomb interaction, for impacts between neutrals – the hard core impact model as shown in Gonzalez et al. (1995), and for ion–neutral impacts – extension of the hard core impact model outside the Debye sphere. We accepted that the

interaction force due to atomic polarisability is proportional to r^{-5} and thus the integral contribution of the core is proportional to r^{-4}. Further, we assumed that the contribution of the core to the collision cross-section of ions is characterized by the factor

$$\phi_j = (1 - \delta_{0j}) D_j^2 / D_0^2, \tag{2.13}$$

where D_j is the diffusion coefficient of the particle in the ionization stage j. The radius of the core in the hard-sphere model has been taken to correspond to the effective main quantum number in the hydrogenic approximation. Thus the total diffusion coefficient for the sum of ions j is

$$\Delta_i = \sum_j (D_0 \phi_j + D_j) X_j, \tag{2.14}$$

where X_j is the ionization fraction corresponding to the subscript.

Excellent analytical approximations and corresponding Fortran code for the calculations of both the Voigt function and its spectral derivative by Humlíček (1979) have been used. These functions are necessary for computations of radiative acceleration (Eq. 2.9) and LID (Eq. 2.11).

Light-induced drift is expected to be most effective in the stellar atmosphere. In stellar interiors heavy elements are highly ionized. Isotopic shifts of lines of high ions are so large that lines of different isotopes do not overlap and thus systematic asymmetry of isotopic lines does not form. In dense plasma radiative flux forms locally and thus asymmetry of flux in spectral line would be anyway smaller than in the atmosphere where asymmetry cumulates over many layers. In outer layers of atmosphere LID efficiency ε is small, because in very rarified plasma the electrons of excited states return to lower states before they collide with other particles.

These considerations lead to the following possible scenario of formation of mercury elemental and isotopic anomalies in HgMn stars. Radiative-driven diffusion in stellar interiors pushes heavy elements (including mercury) to the lower boundary of the atmosphere during stellar evolution. This process have been modelled by Michaud and his colleagues (see Section 1.3.1, Fig. 1.7). Matter entering the atmosphere from beneath has initial (terrestrial) isotope composition. In the atmosphere light-induced drift switches on, effectively separating the isotopes. Observed abundances form in the result of complex interplay between gravity, radiative force, LID, stellar wind and microturbulence.

CHAPTER 3
MODEL COMPUTATIONS

3.1 Evolutionary separation of mercury isotopes

Computations of the evolutionary sequences for abundances of mercury isotopes in several model atmospheres corresponding to CP stars have been made using the Fortran 90 program SMART (Sapar & Poolamäe 2003; Sapar et al. 2007b; Aret et al. 2008).

The model atmosphere data correspond to standard points, being equidistant on the logarithmic scale of the Rosseland mean optical depth. These points are enumerated as layers n growing downwards. Treating n as a continuous parameter, we change variables in equation of continuity (2.2). Since

$$\frac{d}{dr} = \frac{d/dn}{dr/dn} \quad \text{and} \quad \rho\frac{dr}{dn} = -\frac{d\mu}{dn},$$

where μ is total column density, we obtain for radial gradient

$$\frac{d}{dr} = -\gamma\frac{d}{dn}, \quad \text{where } \gamma = \frac{\rho}{d\mu/dn} = \frac{\rho}{\mu d\ln\mu/dn} \ . \tag{3.1}$$

Derivative of logarithm $\ln\mu$ is used in numerical calculations because it changes with depth much slower than column density μ itself. Denoting the ratio of current concentration to its initial value as C_i, we can write $\rho_i = \rho_i^0 C_i$ and the equation of continuity (2.2) reduces to

$$\frac{d\ln C_i}{dt} = \frac{\gamma}{\rho_i}\frac{d(\rho_i V_i)}{dn} \ . \tag{3.2}$$

Logarithms are used to avoid possible negative values of C_i in time integration. Changing variables in equation of diffusion velocity (2.8) we obtain:

$$V_i = D_i\left(\frac{m_i}{kT}(a_i^{\rm rad} - g) + \gamma\frac{d\ln N_i}{dn}\right). \tag{3.3}$$

The velocity V_i is to be used in the equation of continuity (3.2).

As we see, for evolutionary computations we need to find derivatives $d\ln\mu/dn$ and $d\gamma/dn$, which correspond to buffer gases and several derivatives for each isotope of the trace (impurity) particles. The derivatives have been found using the

4th order Lagrange interpolation formulae for equidistant nodes. Boundary conditions were also specified using the Lagrange 4th order interpolation polynomials.

Model computations of LID demand high-precision input physics and precise data on isotopic and hyperfine splitting of spectral lines. Since the overlap of spectral lines is crucial for the LID generation, synthetic spectra must be calculated with high resolution at all atmospheric layers. Due to low values of opacities in the atmosphere, radiative flux is to be found resolving radiative transfer equation at every frequency point. We have found that resolution $\lambda/\Delta\lambda = 5\ 000\ 000$, corresponding to Doppler shift 60 $\mathrm{m\,s^{-1}}$, was necessary to obtain reliable values of LID. This drastically increased expected computation times and forced to search for the possible optimisations of the code.

Another substantial computational problem arises from the fact that diffusion time scales are essentially different in high and deep layers of the atmosphere. Due to much longer free paths in the higher atmospheric layers, diffusive separation proceeds there essentially quicker than in the deeper and denser ones. Diffusion coefficient in upper layers is up to 5 orders of magnitude larger than in deep layers (Fig. 3.1). Consequently, time steps have to be chosen small enough to ensure stability of algorithms in upper layers, but a very large number of time-steps, which is necessary therefore, yields only small changes in deep layers. Considerable efforts have been made to improve stability of algorithms, which would allow to increase time steps and thus reduce the overall computation time.

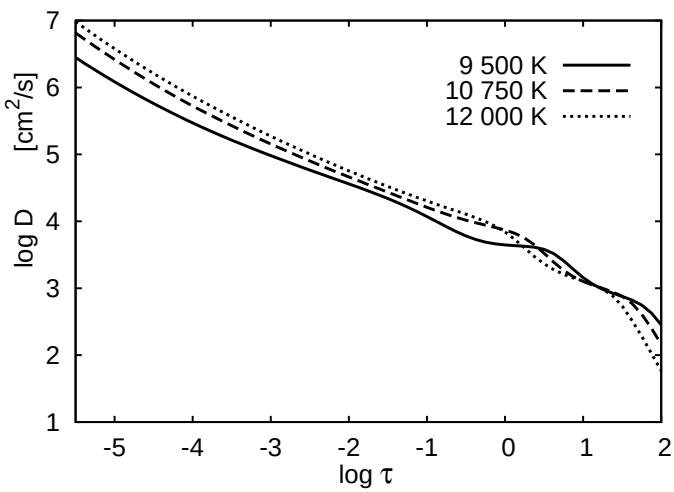

Figure 3.1: Total diffusion coefficient of mercury in model atmospheres with three different temperatures $T_{\mathrm{eff}} = 9\ 500\ \mathrm{K}, 10\ 750\ \mathrm{K}, 12\ 000\ \mathrm{K}$. All model atmospheres are with $\log g = 4, V_{\mathrm{rot}} = 0, V_{\mathrm{turb}} = 0$.

3.2 Software package SMART

Model atmosphere software package SMART (Sapar & Poolamäe 2003; Sapar et al. 2007b; Aret et al. 2008) is a compact and user-friendly software composed for modelling stellar atmospheres and studying different physical processes in them. The codename is acronym of Spectra and Model Atmospheres by Radiative Transfer. Originally composed in FORTRAN 77 it has been essentially improved and refactored to Fortran 90/95 during recent years.

Program SMART enables to compute the plain-parallel and static model stellar atmospheres and corresponding emergent spectra of O, B and A spectral classes in the effective temperature $T_{\rm eff}$ interval from 9 000 to about 40 000 K. Restrictions in modelling are that the atmosphere is chemically homogeneous and that the local thermodynamical equilibrium (LTE) holds.

Upper and lower limits of the effective temperature $T_{\rm eff}$ and gravity $\log g$ are determined by several physical constraints. In software SMART the convective energy transport is neglected and molecular absorption only by H_2 and H^- is taken into account. This sets constraint to the lowest effective temperature. The highest $T_{\rm eff}$ is restricted primarily by need to take more adequately into account wide profiles of frequency redistribution in spectral lines, generated due to multiple scattering of radiation on free electrons. The lower limit of $\log g$ at given effective temperature is set by the Eddington limit of stability of stellar atmospheres. Upper limit of $\log g$ is determined by circumstance that at large densities corresponding to the large values of $\log g$ in white dwarfs, the contribution of the linear Stark effect to the Voigt line profile of hydrogenic species (i. e. H and He^+) differs essentially from the used electrostatic Holtsmark profile. Holtsmark approximation is acceptable for ions but not for the rapidly moving electrons (Griem et al. 1959). Since HgMn stars are located on the main sequence ($\log g \approx 4$) in the interval of the effective temperatures $T_{\rm eff} \approx$ 9 500 K – 14 000 K, they belong to the temperature–gravity region adequately treated by SMART.

The capabilities of the program SMART are quite wide. Main code for atmosphere modelling and computation of emergent stellar flux provides iterative correction of initial model atmosphere and gives detailed radiative flux in all layers of the atmosphere. Specific tasks of SMART include computations of evolution of diffusive separation of isotopes in atmospheres of CP stars, relaxational formation of NLTE in line spectra, accelerations of clumps in stellar atmospheres triggering stellar wind, computation of detailed spectral limb darkening and hence the spectra of rotating stars and non-irradiated eclipsing binaries. Pan-spectral method for determining element abundances from high-quality observed spectra have been developed and implemented as an extension to SMART.

3.2.1 Structure

General structure of the program SMART is shown in Fig 3.2.

Initial block

Initialization. Read program control specifiers and delimiters. Determine specific task of current run. Initialize data arrays with common atomic etc. data.

Read model. Read in model atmosphere data and process them according to the present task. Kurucz (1993a) model atmospheres are input data for model correction task. Other tasks use model atmospheres previously computed by SMART.

Start arrays. Form arrays of data necessary to start the main block.

Read linelist. Read line list `gfhyperall.dat` by R. Kurucz (obtained from his web page http://kurucz.harvard.edu/) and list of Hg lines compiled by us. Lines needed for computations in given spectral interval are selected according to the cut-off delimiter of value $gfA_Z e^{h\nu/kT_{\rm eff}}$, where A_Z is number abundance of element Z and gf is a line strength. Large spectral interval is divided into smaller sections with constant resolution $R = \nu/\Delta\nu$ and line list is composed for every section. Computations in the main block loop over these sections.

Main block

Saha. Compute ionization rates and partition functions for all ions. Diffusion coefficients are also computed there.

Continuous absorption. The absorption cross-sections for most of continua are computed using a variant of Seaton formula in the form $\sigma = \sigma_0 \sum_i^3 \alpha_i (\nu/\nu_0)^{\beta_i}$, where σ_0 is the absorption cross-section at the threshold of the continuum and ν_0 is the corresponding photon frequency. α_i and β_i are the fitting constants. For the hydrogen states the usual Kramers formula with more exact Gaunt factors is used. The most problematic task is to take adequately into account formation of the pseudo-continua in the region of Rydberg states. In this spectral region the corresponding Inglis-Teller type switch-in of continua has been applied, which guarantees smooth transition from line series to corresponding continua. Continuum opacities are computed at each wavelength step.

Line absorption. Line opacity is computed for all spectral lines in each spectral section at each model atmosphere layer. The Voigt line profile function has been used for non-hydrogenic spectral lines and for hydrogenic spectral lines also an averaged linear Stark effect has been incorporated in the Holtsmark approximation. In addition to the Voigt function, its derivative with respect to the wavelength needed for LID computations, is found. In the case of diffusion task, contribution

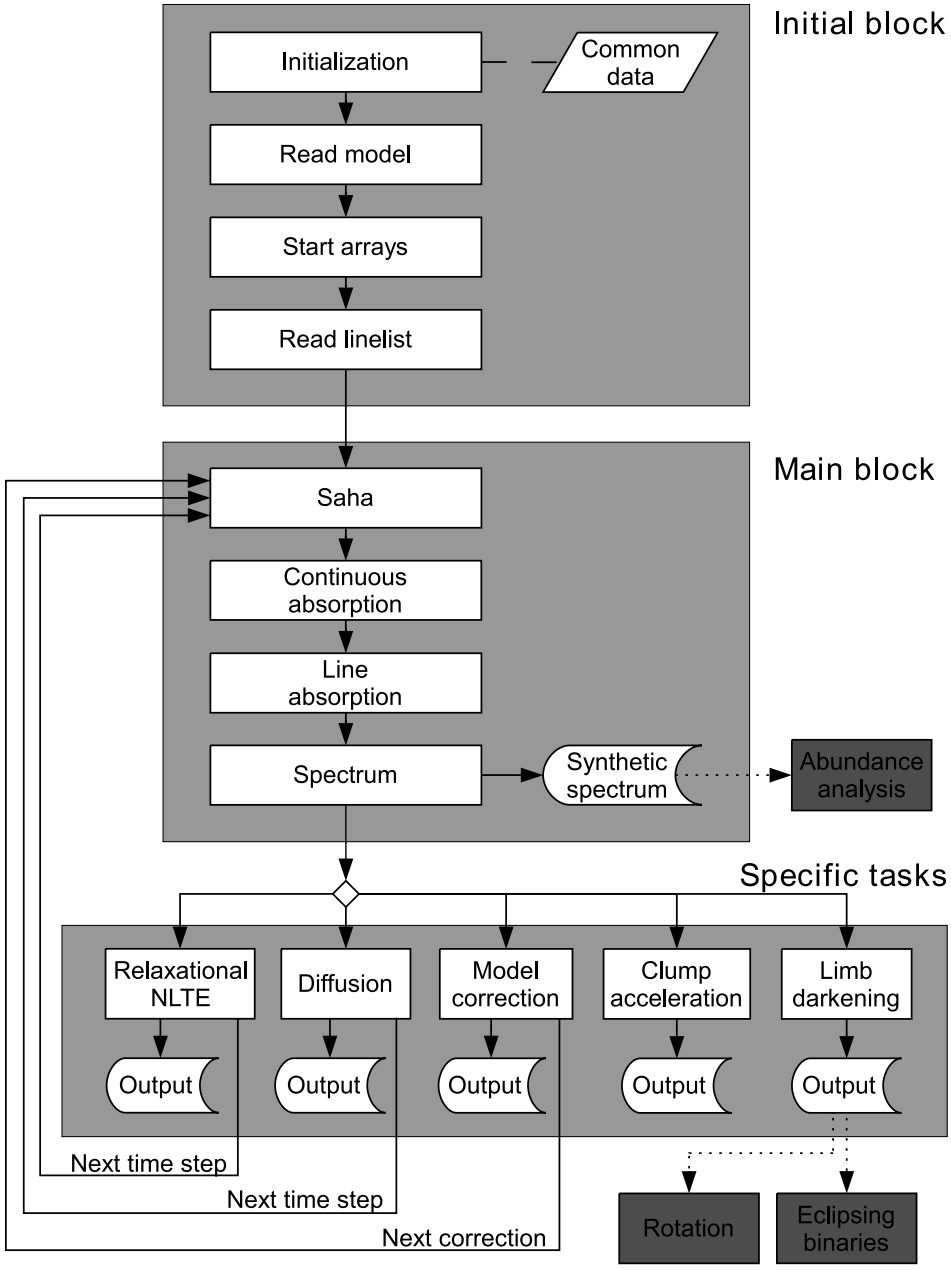

Figure 3.2: General structure of program SMART.

of every line to the usual radiative acceleration and to the LID acceleration is calculated. For NLTE computation, the corresponding Menzel correction coefficients of state population are included.

Spectrum. Radiative transfer from layer i has been calculated using integration by parts inside each layer L, yielding series of exponential integrals over monochromatic optical depths τ:

$$\int fE_n(\Delta+s\tau)d\tau = -sfE_{n+1}(\Delta+s\tau)-f'E_{n+2}(\Delta+s\tau)-sf''E_{n+3}(\Delta+s\tau), \tag{3.4}$$

where $\Delta = |\tau_L-\tau_i|$; $s = -1,$ if $i < L$; $s = 1,$ if $i \geq L$. The scattering processes are computed by simple Λ-iteration. Radiative transfer calculations give radiative flux $F_\nu(\tau_i)$ in all layers of atmosphere.

Specific tasks

Relaxational NLTE. Relaxational formation of NLTE in spectral lines is calculated by uniformly converging time-step iterations. Equilibrium quantum state populations of ion states are found from the equations of unbalanced statistical equilibrium treated as an relaxational initial value problem from LTE to NLTE populations. Instead of Λ-iterations, a physically changing emissivity (or the source function) is used. The relaxation scheme incorporates changing Menzel coefficients for NLTE quantum state populations. This computational scheme is essentially simpler and more compact than any linearisation scheme.

Diffusion. Time-dependent diffusion of isotopes of a selected element is calculated taking into account radiative acceleration, light-induced drift and gravity according to the formulae given in Chapter 2 and Section 3.1. In the present thesis computations have been made for mercury isotopes in HgMn stellar atmospheres.

Model correction. Model atmospheres are improved iteratively, varying only temperature and pressure dependency on column density. The radiative flux is computed as in the synthetic spectrum calculations without any additional simplification of absorption and scattering in spectral lines. Flux constancy 0.1–0.5 % is achieved by about 10 iterations, using Kurucz (1993a) ATLAS9 models as input. Number of atmospheric layers can be multiplied if necessary.

Clump acceleration. Radiative acceleration of the moving turbulent clumps in stellar atmosphere is computed. This enables to connect the model atmosphere computations with the problem of the stellar wind triggering.

Limb darkening. Spectral limb darkening is computed. Obtained data is used for calculating spectra of rotating stars and non-irradiated eclipsing binaries.

Extensions

Abundance analysis. Computation of element abundances in CP stars by a new pan-spectral method (Sapar et al. 2008a) aimed for the automatic processing of high-quality stellar spectra. The method is based on weighted cumulative line-widths Q_λ defined as

$$Q_\lambda = \int_{\lambda_0}^{\lambda} \left| \frac{dR_\lambda}{dZ} \right| (1 - R_\lambda) d\lambda \ ,$$

where R_λ is the residual flux (intensity) and $Z = \log(N_{\rm elem}/N_{\rm tot})$ is the abundance of studied chemical element or its isotope. The derivative of residual flux R_λ with respect to abundance Z automatically excludes spectral regions insensitive to changes of the abundance of studied element and gives a large contribution in the most sensitive regions, i. e. in the centres of non-saturated lines and in the steep wings of strong lines of the element. Best fit of quantities Q_λ found from synthetic and observed spectra gives final abundance, taking duly into account all lines of a studied element including blended ones. Abundances can be found simultaneously for many elements. This method can also be used to find corrections to the effective temperature and gravity.

Rotation. Computation of spectra of rotating stars using detailed spectral limb darkening data obtained with SMART. The additional Doppler shift due to rotation is taken into account integrating over the stellar disk. Dependence of the effective temperature on the latitude is incorporated for fast rotating stars by the von Zeipel theorem.

Eclipsing binaries. Computation of spectra of non-irradiated eclipsing binaries using detailed spectral limb darkening data obtained with SMART. The eclipsed part of the stellar disk is excluded. Both the rotational and tidal deformations of stellar disk are taken into account if necessary.

3.3 Input data for LID computations

Spectral line data for mercury have been compiled using different sources and improved by adding isotopic splitting to all available Hg lines. Most of the line data have been taken from the lists by Kurucz & Bell (1995) and Vienna atomic line database VALD (Kupka et al. 2000). Hyperfine and isotopic structure of Hg lines and their oscillator strengths available in papers by Proffitt et al. (1999) and Smith (1997) were used to improve our line list. For other lines isotopic splitting was calculated using relative shifts found by Striganov & Dontsov (1955), scaled to units $[202 - 200] = 1$, giving for other splitted line components

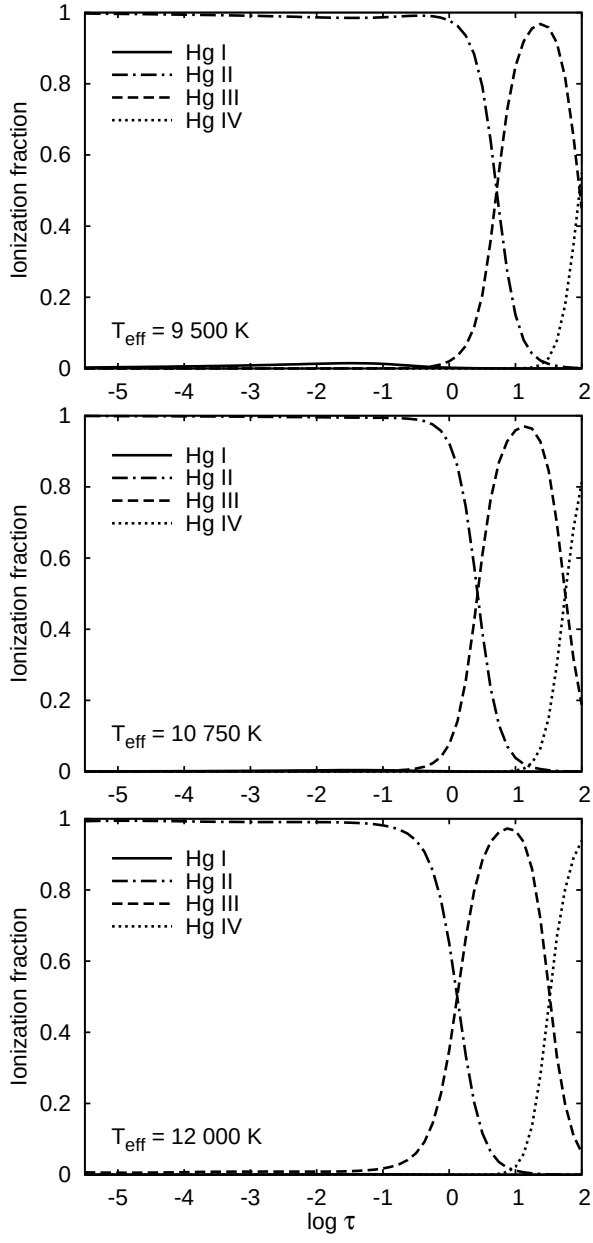

Figure 3.3: Ionization fractions of mercury ions in model atmospheres with three different temperatures $T_{\rm eff}=$ 9 500 K, 10 750 K, 12 000 K and $\log g = 4$, $V_{\rm rot} = 0$, $V_{\rm turb} = 0$.

12

$[198-200] = -0.94$, $[199-200] = -0.80$, $[201-200] = 0.30$, $[204-200] = 1.98$. For scaling these relative shifts to wavenumbers, we have taken into account that $[202-200] = 0.179$ cm^{-1} for Hg I, $[202-200] = 0.508$ cm^{-1} for Hg II and $[202-200] = 0.600$ cm^{-1} for Hg III. Compiled line list contains about 700 resonance and low excitation spectral lines in the wavelength range from approximately 800 Å to 12 000 Å for Hg I, Hg II and Hg III, i. e. for ion species, which are most important for LID. However, for deeper layers of stellar atmospheres also the line data for Hg IV is necessary (Fig. 3.3) which is not available at the present time. But on the other hand, isotopic shift in Hg IV lines is so large that they do not overlap and systematic asymmetry of isotopic lines does not form. Therefore the contribution of Hg IV lines to the LID is probably inessential.

Model atmospheres for evolutionary computations have been computed with SMART, using sampling for moderate spectral resolution ($R = 30\ 000$). Spectral line data from Kurucz file `gfhyperall.dat` (obtained at http://kurucz.harvard.edu/) have been used in these computations. Model atmospheres have not been recalculated during evolutionary computations. Since mercury is just a small admixture, even large change of its abundance cannot have essential effect on the atmospheric structure.

CHAPTER 4
RESULTS OF MODEL COMPUTATIONS

Formation of evolutionary stratification of Hg isotopes has been computed for a set of model atmospheres with three effective temperatures ($T_{\rm eff}$ = 9 500 K, 10 750 K, 12 000 K) and three initial Hg abundances (ρ^0 = solar, solar + 3 dex, solar + 5 dex), all with $\log g = 4$. For atmosphere modelling of these quiescent stars the rotation velocity $V_{\rm rot}$ has been assumed to be zero and the microturbulence, which can essentially decelerate the process of separation and diminish the final radial gradient of light isotope abundances, has been ignored ($V_{\rm turb} = 0$). Possible presence of stellar wind, reducing or even cancelling the diffusional separation of isotopes, has also been ignored.

Solar system abundance of mercury $\log(N_{\rm Hg}/N_{\rm tot}) = -10.91$ has been adopted (Asplund et al. 2005). Homogeneous initial abundance of Hg throughout the atmosphere and initial solar system (terrestrial) ratios of isotope abundances (Rosman & Taylor 1998) have been used.

The longest evolutionary sequence (6 500 time steps, à 1 year) has been computed for model atmosphere with parameters $T_{\rm eff} = 10\ 750$, $\log g = 4$, $V_{\rm rot} = 0$, $V_{\rm turb} = 0$ and initial Hg abundance solar + 5 dex corresponding to the atmosphere of HgMn star HR 7775 (Dolk et al. 2003).

4.1 Accelerations of mercury isotopes

Model computations by the code SMART confirmed dominant role of LID in separation of isotopes of heavy elements in chemically peculiar stellar atmospheres. Radiative acceleration $a^{\rm rad}$ is almost the same for all isotopes, whereas effective acceleration due to LID is drastically different for different isotopes.

The initial acceleration profile throughout the stellar atmosphere has been demonstrated in Fig. 4.1 for the solar, solar + 3 dex and solar + 5 dex abundances of mercury and solar system ratio of its isotopes. Accelerations of the mercury isotopes ^{198}Hg (the lightest[1]) and ^{204}Hg (the heaviest) are shown. Main parameters of the model $T_{\rm eff} = 10750$ K and $\log g = 4$ in CGS units are typical for chemically peculiar stellar atmospheres.

Modified logarithmic scale

$$\mathrm{logm}\left(\frac{a}{g}\right) = \mathrm{sign}(a)\log\left(\left|\frac{a}{g}\right| + 1\right) \tag{4.1}$$

[1]The isotope ^{196}Hg has been ignored due to its very low abundance (Table 1.1)

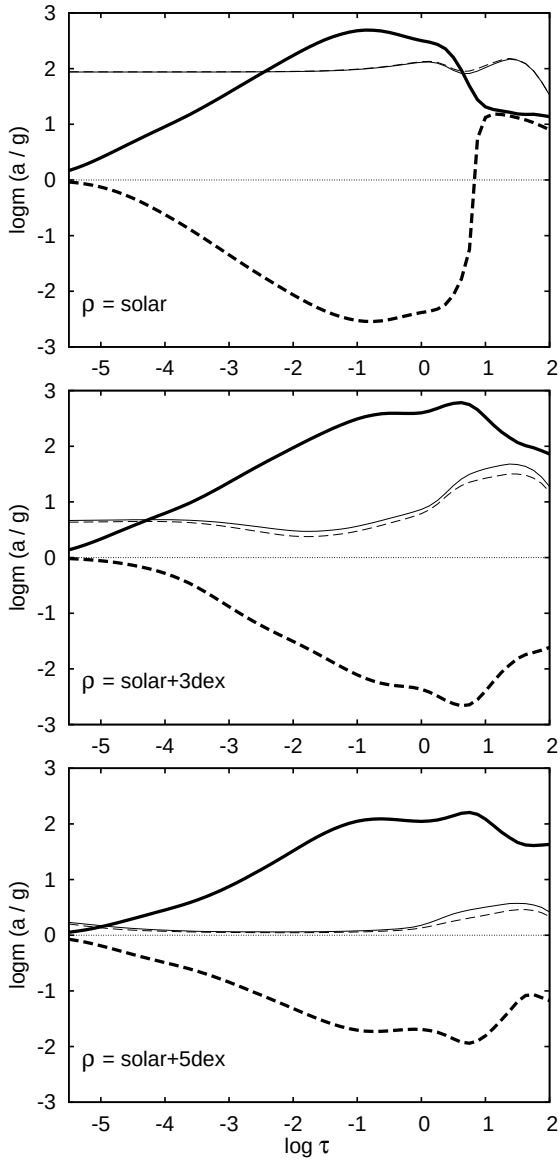

Figure 4.1: Accelerations a^{rad} (thin line) and a^{LID} (thick line) of mercury isotopes ^{198}Hg (dashed line) and ^{204}Hg (solid line) at first time step (i.e. with homogeneous Hg abundance) for solar, solar + 3 dex and solar + 5 dex abundances of mercury and solar system isotope ratio. Accelerations a^{rad} and a^{LID} are given relative to gravity g and represented in the modified logarithmic scale (Eq. 4.1). Model atmosphere $T_{\mathrm{eff}} = 10\,750$ K, $\log g = 4, V_{\mathrm{rot}} = 0, V_{\mathrm{turb}} = 0$.

has been used to represent a sign-changing acceleration and to obtain different scaling for small and large values of the functions studied. Such scale is almost logarithmic at large values of function and almost equal to it at its small values. This enables to represent in a figure a run of sign-changing quantities varying in a wide range of values.

In outer layers of the atmosphere radiative acceleration is dominant, because in very rarified plasma the electrons of excited states return to lower states before they collide with other particles and thus the LID efficiency ε is small (Eq. 2.12).

The effective acceleration of mercury isotopes due to the LID cannot be expected to be large in the case of solar abundances of isotopes, because blending with strong neighbouring lines is more important than mutual influence of very weak partially overlapping lines of mercury isotopes. However, even in this case in deeper layers of atmosphere $a^{\rm LID}$ turned out to be of the same order of magnitude as $a^{\rm rad}$.

The larger is mercury abundance, the more important is LID. Mercury lines in model atmosphere with high mercury abundance (solar + 5 dex) are strong and the mutual influence of overlapping isotope lines is dominant, generating large light-induced drift. Effective acceleration due to the LID exceeds radiative acceleration up to 2 dex, determining the total acceleration of mercury isotopes. As expected, the acceleration due to LID is directed downward for lightest isotope ^{198}Hg and upward for the heaviest ^{204}Hg. Both the downward and upward directed accelerations grow with optical depth τ up to $\tau = 10$. Decrease of $a^{\rm LID}$ in deeper layers can be caused by two reasons. First, spectral line splitting is larger for higher stage ions and thus the mutual overlap of isotope spectral lines decreases. Second, fraction of Hg III becomes important in those layers, but spectral line data for Hg III has been since not available.

4.2 Scenario of evolutionary separation of isotopes

Computed evolutionary scenarios demonstrated rapid changes in the total acceleration due to LID and presence of relaxational damping of isotopes flow. The evolutionary changes of the Hg total acceleration profiles in the quiescent stellar atmosphere with main parameters $T_{\rm eff} = 10750$ K, $\log g = 4$ and initial mercury abundance solar + 5 dex with solar system isotope ratios are shown in Fig. 4.2. As we see, the total radiative acceleration for the heaviest and for the lightest isotope changes with time much less than for the rest intermediary atomic weight isotopes which undergo large and complicated changes but finally acquire similar acceleration profiles with the lightest isotope throughout the stellar atmosphere. The dominant part of the acceleration in the outer layers of stellar atmosphere is

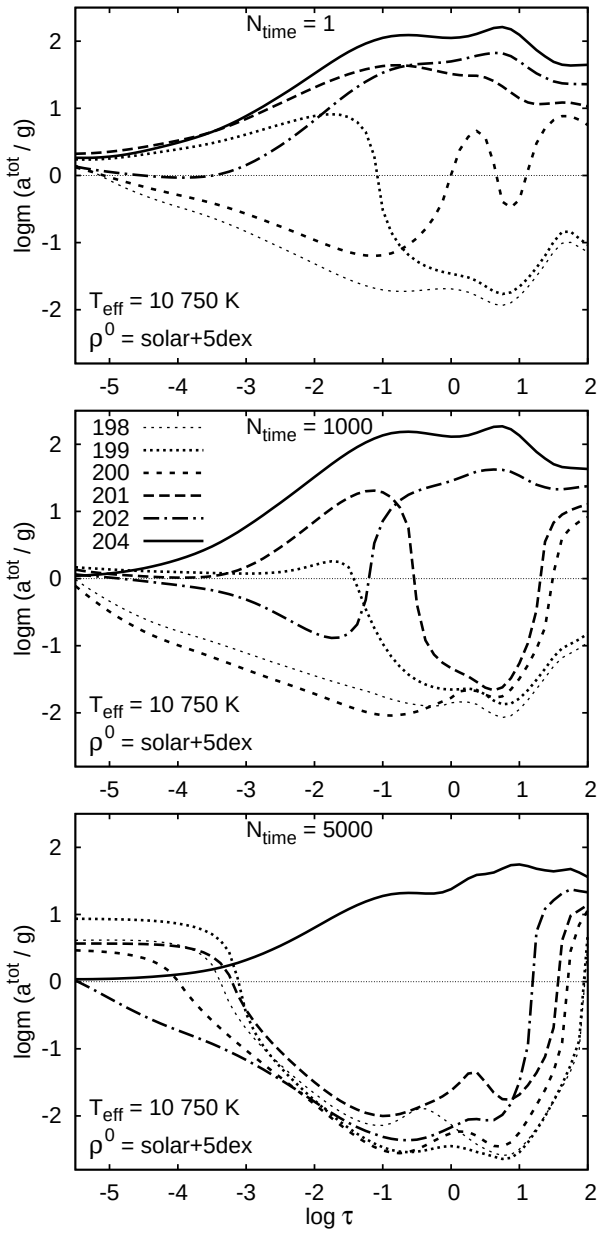

Figure 4.2: Change of acceleration $a^{\rm tot} = a^{\rm rad} + a^{\rm LID}$ from the first to the 5000th time-step. The ratio $a^{\rm tot}/g$ is given in the modified logarithmic scale (Eq. 4.1). Note the complicated change of the curves for intermediary isotopes.

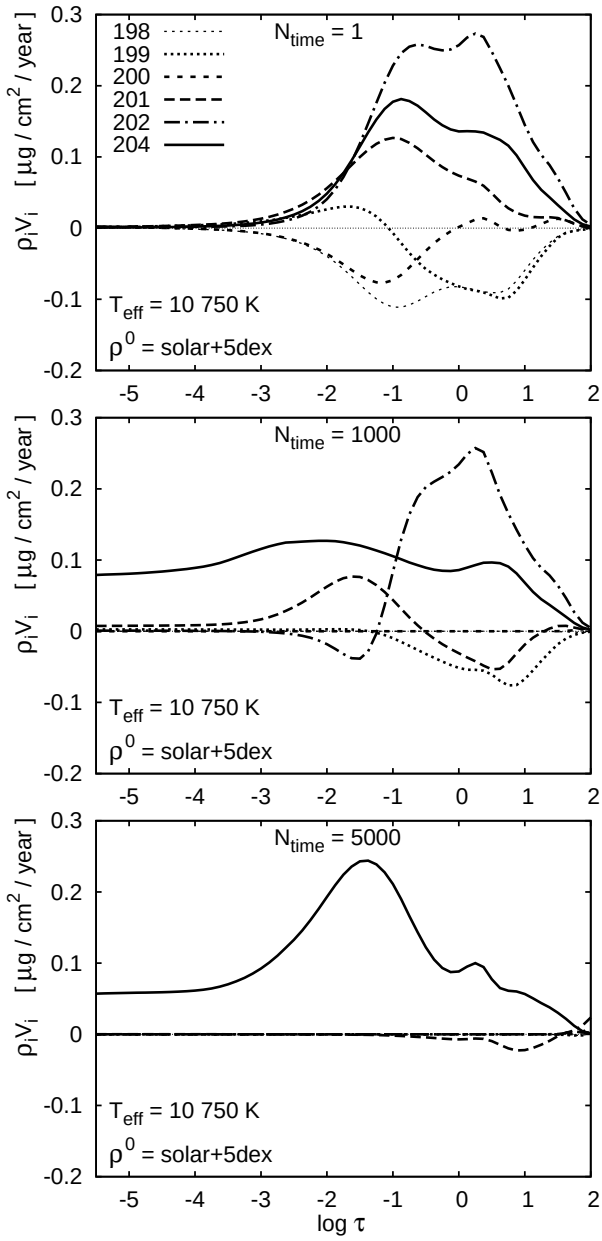

Figure 4.3: Change of flows of Hg isotopes from the first to the 5000th time-step. Note the evolutionary damping of the flows.

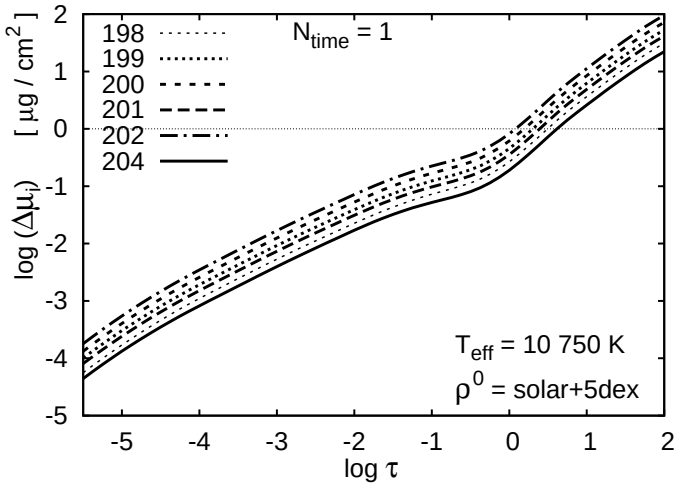

Figure 4.4: Column densities of Hg isotopes in model atmosphere layers with parameters $T_{\rm eff} = 10\ 750$ K, $\log g = 4, V_{\rm rot} = 0, V_{\rm turb} = 0$, for Hg abundance solar+5 dex and solar system isotope ratios at the first time step (i.e. with homogeneous Hg abundance).

given by Hg I, in the middle part of the optical depths by Hg II and in the deepest layers by the Hg III ions.

The evolutionary changes in the isotope flows at the same moments as the accelerations in Fig. 4.2 are depicted in the Fig. 4.3. We can see that evolutionary damping of the flows is most rapid for isotopes with lower even mass number, followed by the odd isotopes ^{199}Hg and ^{201}Hg. Spectral lines of these odd-A isotopes in addition to the isotopic splitting undergo also the hyperfine splitting, which causes increase of the radiative acceleration $a^{\rm rad}$ of these isotopes and changes of $a^{\rm LID}$ for all isotopes due to mixing of the spectral order of isotopic lines (see Section 4.5). The flow of the heaviest isotope ^{204}Hg remains considerable for the longest time. Comparison of isotope flows with column densities of these isotopes in model atmosphere layers (Fig. 4.4) gives an idea of time scales of abundance changes. Separation of isotopes occurs in thousands of years in deep atmospheric layers and much faster in upper layers. These time scales are essentially shorter than evolutionary time scales on the main sequence.

The total radiative acceleration rules the sedimentation of lighter isotopes and the levitation of the heaviest isotope. The isotope separation appears first in the outer layers of stellar atmospheres, diluting rapidly the lighter even-A isotope abundances (Fig. 4.5). This rapid sedimentation propagates downward until ^{198}Hg and ^{200}Hg are heavily diluted throughout the atmosphere. The complicated inter-

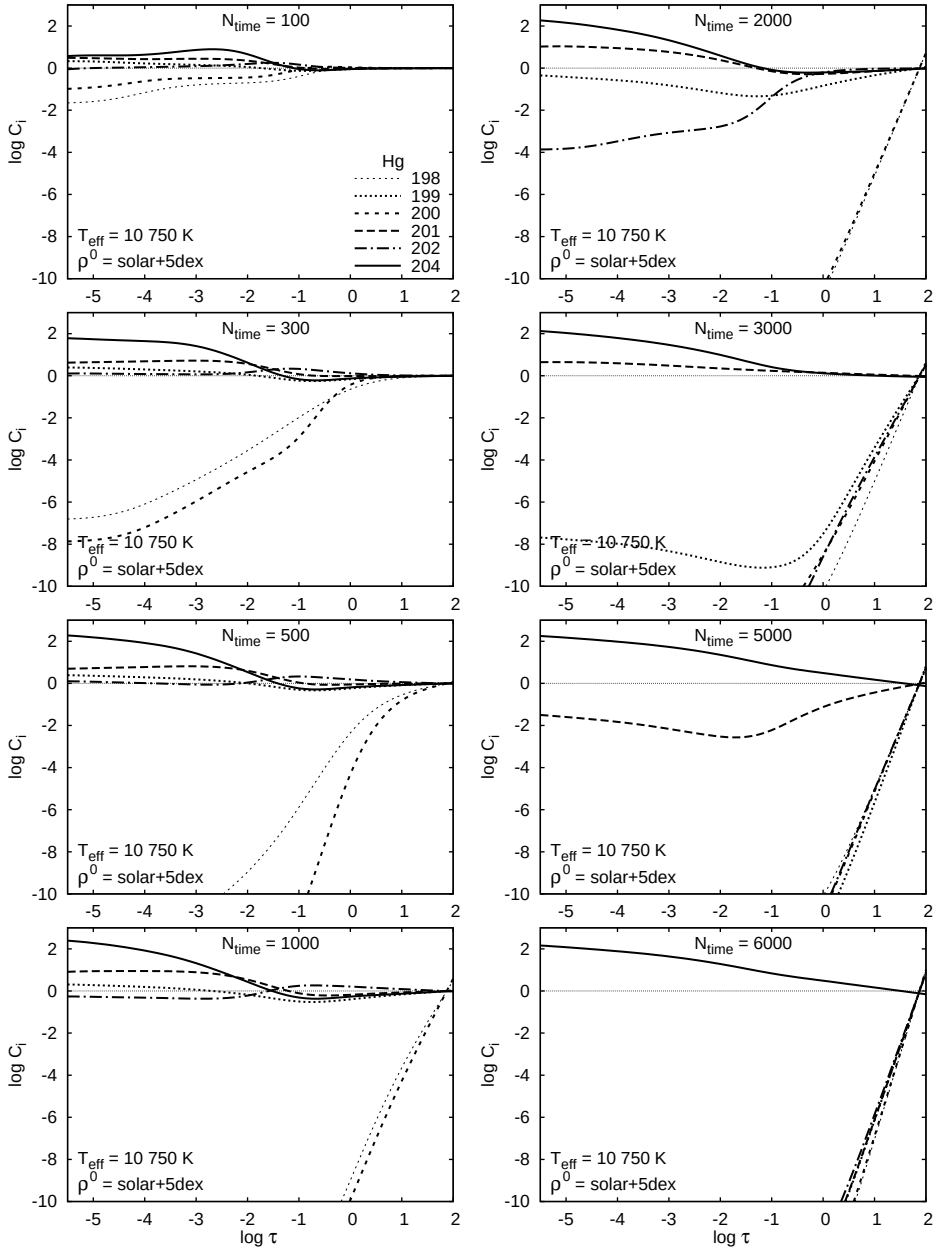

Figure 4.5: Evolutionary changes of mercury concentrations in model atmosphere with $T_{\rm eff} = 10\ 750$ K, $\log g = 4$, $V_{\rm rot} = 0$, $V_{\rm turb} = 0$ and initial Hg abundance solar + 5 dex with solar system isotope ratios.

14

play between odd-A isotopes ^{199}Hg and ^{201}Hg and heavier even-A isotopes ^{202}Hg and ^{204}Hg leads finally approximately to the same equilibrium dilution gradient as for ^{198}Hg and ^{200}Hg. Resulting gradients are obviously too abrupt, because microturbulent mixing has been completely ignored.

Evolutionary changes of Hg II λ3984 Å line are shown in Fig. 4.6. No instrumental broadening has been added to the synthetic profile. Since both microturbulence and stellar rotation also have been ignored, the lines of isotopes are extremely sharp.

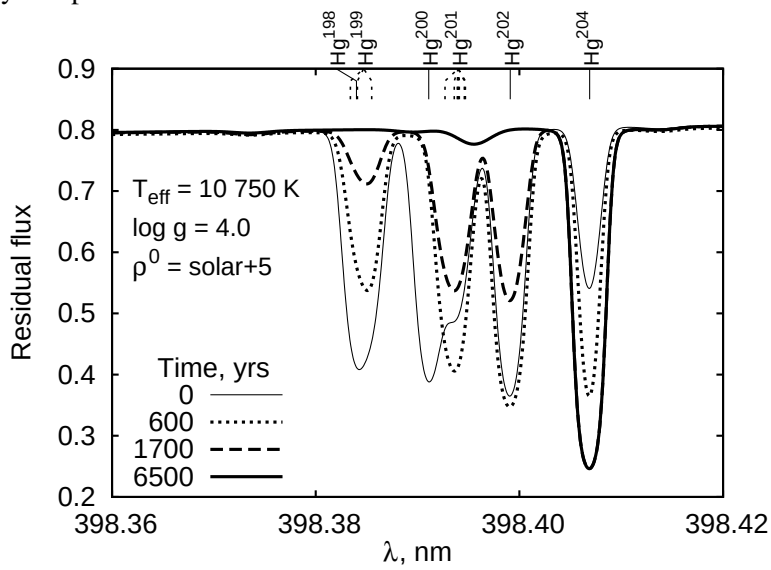

Figure 4.6: Evolutionary changes of Hg II line λ3984 Å. Initial isotope ratios correspond to solar system values.

4.3 Dependence on effective temperature

Evolutionary scenarios of mercury isotope separation have been compared in model atmospheres of main sequence stars with the values of main parameters $\log g = 4$, $V_{\rm rot} = 0$ and C_0 = solar + 5 dex and three effective temperatures, namely 9 500, 10 750 and 12 000 K, which cover most important region of chemically peculiar HgMn stars. The dependence of evolution of Hg concentration on effective temperature $T_{\rm eff}$ is illustrated on Fig. 4.7. Separation of isotopes proceeds much slower at higher effective temperatures. In atmospheres with higher temperatures free-flight time of plasma particles is smaller, leading thus to the smaller diffusion velocities. Another reason for the slower diffusion at higher

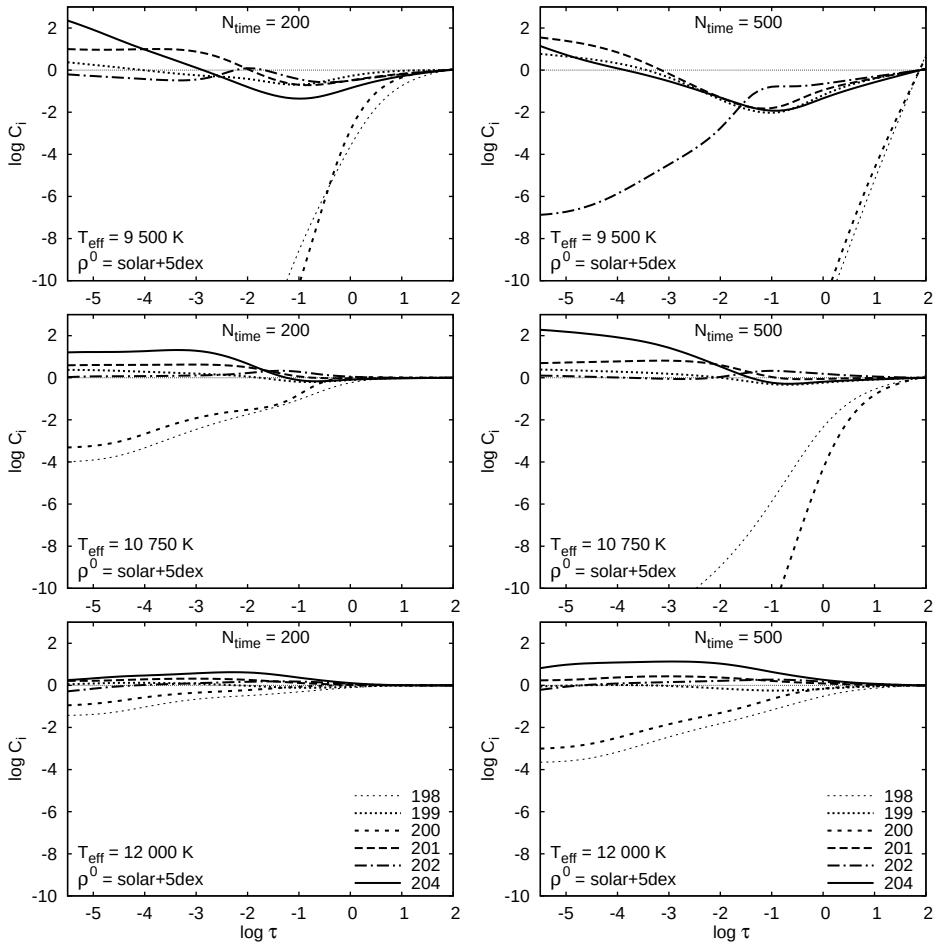

Figure 4.7: Temperature dependence of evolutionary changes of mercury isotope concentrations in model atmosphere with three different effective temperatures $T_{\rm eff} = 9\ 500, 10\ 750$ and $12\ 000$ K. Other model atmosphere parameters in all panels are the same: $\log g = 4, V_{\rm rot} = 0, V_{\rm turb} = 0$. The initial Hg abundance is solar + 5 dex with solar system isotope ratios. Left column: time=200 yr, right column: time=500 yr. Note the essential brake of the separation at higher $T_{\rm eff}$.

temperatures is a lack of neutral mercury, which has about 100 times larger diffusion coefficient than ionized particles.

The lower temperature boundary for diffusion-generated chemically peculiar stellar atmospheres is determined by appearance of the atmospheric convective zone which violently mixes the atmosphere and cancels all diffusion phenomena.

4.4 Dependence on initial mercury abundance

Stellar evolution model computations for various CP stars have shown (Richer et al. 2000; Michaud et al. 2005, 2008; Michaud & Richer 2008) that due to presence of large number of relatively low excitation states and large number of allowed radiative transitions in the spectra of metals, in particular of the heavy metals, radiation-driven diffusion wipes them out from stellar interior regions between 10^{-4} and 10^{-7} of the stellar mass pushing them to the exterior regions (Fig. 1.7). The computed depletion for Fe and Ni in the quiescent interiors is about 20 %, giving overabundance of these metals in the outer envelope about 200 times. Model computations have shown, that the heavier the metal, the deeper extends the region of depletion and the larger is the overabundance in the outer layers. Thus, we can expect the final evolutionary overabundance for Hg up to 10^5 at the lower boundary of the overlaying atmosphere. The radiative acceleration is almost the same for all isotopes and light-induced drift is inefficient in deep layers, so isotopic composition of mercury rising from stellar interiors remains unaffected. Further separation of the isotopes in atmospheric layers is studied in the present thesis.

The dependence of evolution of Hg isotope concentrations on the initial Hg abundance is illustrated in Fig. 4.8. Radiative acceleration is dominant at solar abundance of Hg, the role of LID increases with increase of Hg abundance and it becomes dominant throughout the atmosphere at Hg abundance about solar + 5 dex. In the beginning of the evolution process in the stellar atmosphere with solar abundances of mercury isotopes, the radiative drive is dominant (Fig. 4.8), causing rise of abundance of all Hg isotopes. In outer layers this process is much faster than in deeper layers of the atmosphere. As Hg abundance increases, also the LID increases, causing levitation of heavier and sedimentation of lighter isotopes. Diffusion processes in the case of initial solar abundances turned out to be more than 100 times faster than in atmosphere with initial Hg abundance $\log N_{\mathrm{Hg}}$ = solar + 5 dex. Therefore we took different time steps for different initial abundances, namely

- $\Delta t = 0.01$ yr for initial abundance ρ^0 = solar;
- $\Delta t = 0.1$ yr for initial abundance ρ^0 = solar + 3 dex;
- $\Delta t = 1$ yr for initial abundance ρ^0 = solar + 5 dex.

In reality probably all of these cases can be considered as the initial ones depending on the amount of mercury rising from stellar interiors. Thus, the observed picture of isotope abundances in stellar atmospheres depends also on the ages of the stars.

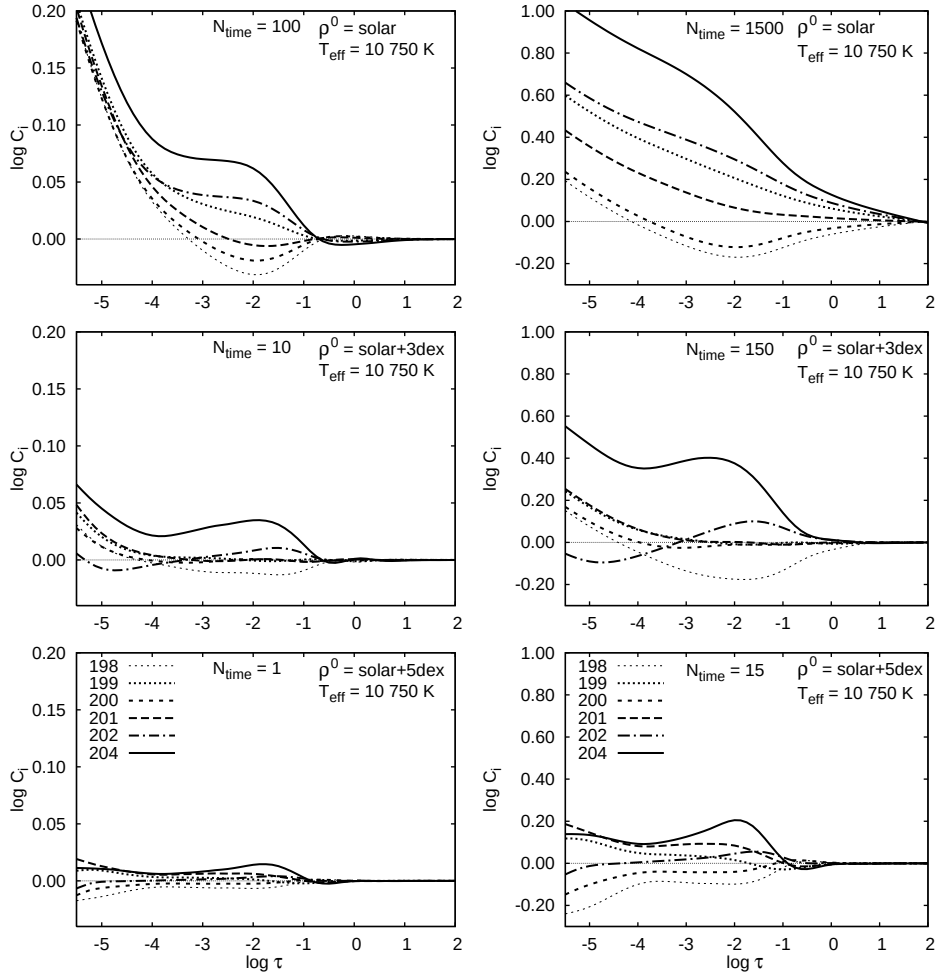

Figure 4.8: Initial abundance dependence of evolutionary changes of mercury isotope concentrations in model atmospheres with three initial abundances ρ^0: solar, solar + 3 dex and solar + 5 dex (all with solar system isotope ratio). Other model atmosphere parameters in all panels are the same: $T_{\rm eff} = 10\,750$, $\log g = 4$, $V_{\rm rot} = 0, V_{\rm turb} = 0$. Left column: time = 1 yr, right column: time = 15 yrs. Note the essential brake of the separation rate at higher initial Hg abundances.

15

4.5 Role of hyperfine splitting of Hg spectral lines

To test the effects of hyperfine splitting of Hg lines on isotope separation, an evolutionary scenario has been computed also for the "pure mercury" case, where lines of all other elements were ignored. This theoretical experiment has been performed to isolate effects of hyperfine splitting.

Evolutionary scenarios for "pure mercury" have been computed for model atmosphere with parameters $T_{\rm eff} = 10\ 750$ K, $\log g = 4$ and initial Hg abundance solar + 3 dex with solar system isotope ratios. First, we carried out "pure isotopic" computations, ignoring the hyperfine splitting of Hg spectral lines, i. e. the hyperfine components of ^{199}Hg and ^{201}Hg were combined into one isotopic component for each line. In the second run, "hyperfine isotopic" computations were made, taking into account both isotopic and hyperfine splitting of spectral lines. The results of the evolutionary computations are illustrated in Fig. 4.9.

Data on hyperfine splitting (Proffitt et al. 1999; Smith 1997) was available for 14×2 lines out of 99×2 lines of ^{199}Hg and ^{201}Hg. Structure of isotopic and hyperfine splitting of strong Hg II line λ3984 Å is illustrated in Fig. 4.6.

The hyperfine splitting acts in two ways. First, it reduces saturation in the spectral lines of odd-A isotopes. This causes essential increase of the radiative acceleration $a^{\rm rad}$ supporting these isotopes in the atmosphere. Similar result has been also obtained for ^{201}Hg by Woolf & Lambert (1999). Amplification of $a^{\rm rad}$ is stronger for ^{201}Hg reaching 400% in layers near $\tau \sim 0.01$. Second effect is that hyperfine splitting entangles the order of isotope lines affecting LID acceleration $a^{\rm LID}$ of all isotopes, particularly of the intermediate isotopes ^{199}Hg, ^{200}Hg and ^{201}Hg (Fig. 4.10).

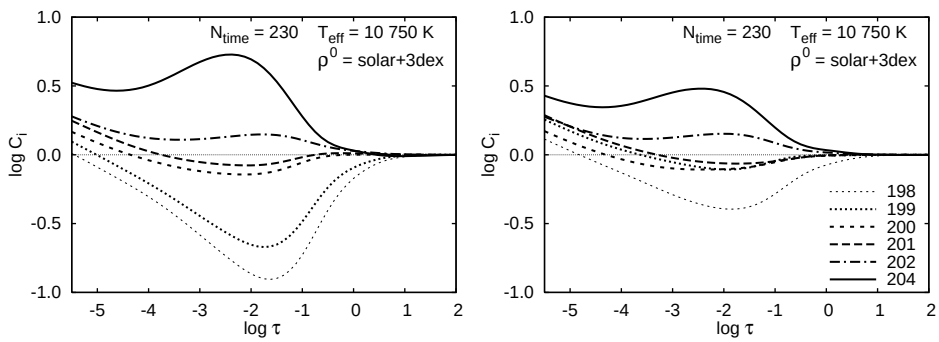

Figure 4.9: Evolutionary changes of "pure mercury" concentrations without hyperfine splitting (left panel) give the uncrossed curves in the order of isotope masses and with hyperfine splitting (right panel) give slower diffusion and intersecting curves for intermediate isotopes.

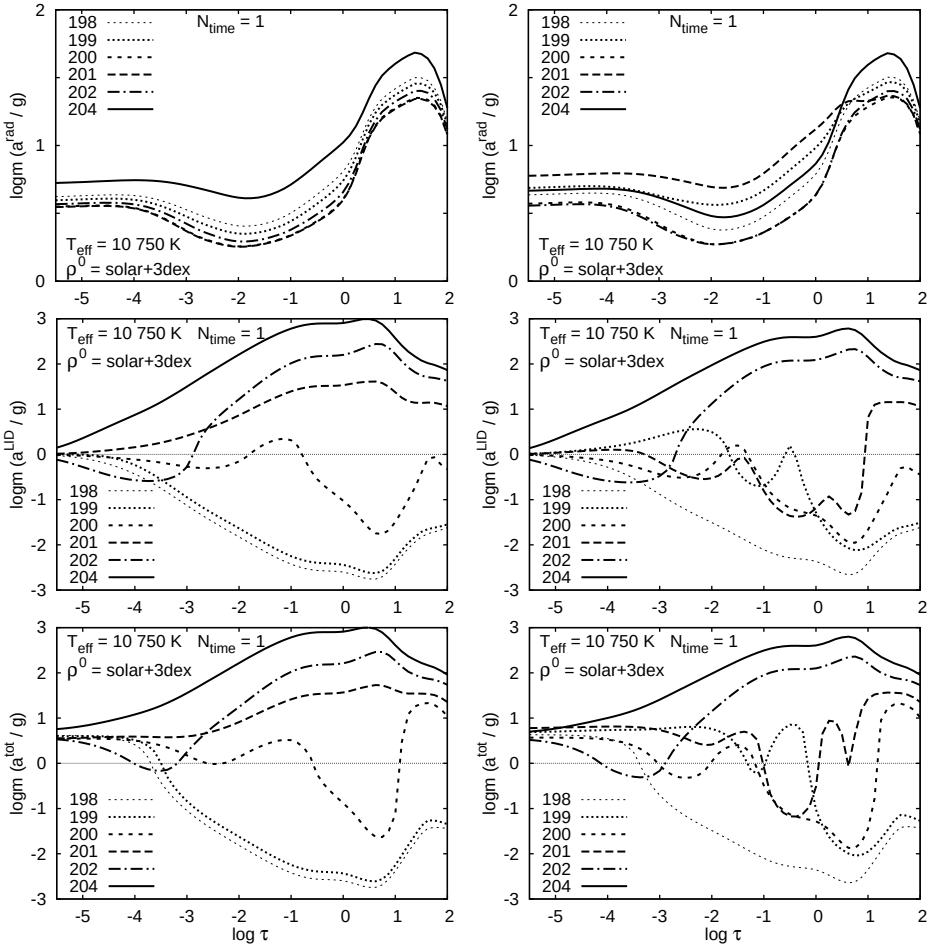

Figure 4.10: Accelerations a^{rad}, a^{LID} and $a^{\mathrm{tot}} = a^{\mathrm{rad}} + a^{\mathrm{LID}}$ on "pure mercury" in model atmosphere with homogeneous Hg distribution without hyperfine splitting (left panels) and with hyperfine splitting (right panels) of spectral lines of odd-A isotopes ^{199}Hg and ^{201}Hg.

In "pure isotopic" case isotopes are separated in the order of their masses: lighter isotopes sink and heavier ones rise. Hyperfine splitting of spectral lines of odd isotopes evokes more complicated picture of evolutionary changes of isotope abundances. It also affects separation time scales slowing down the diffusion process. Difference between these two cases would be somewhat larger if a more complete line list were used. It is evident that complete and precise line lists and detailed model computations are necessary for studies of LID.

4.6 Mercury in the atmospheres of observed HgMn stars

Results of detailed analysis of the mercury isotope abundances in 30 HgMn stars have been reported by Dolk et al. (2003). Determined abundances are given in Table 1.1. The observed stars can be divided into three groups:

I group

Three stars 56 Aqr, HR 7361, and θ Hyi have Hg abundances enhanced by about 5 dex and solar isotope ratios. These stars have the largest observed component values of rotation velocity $V_{\rm rot} \sin i$ among program stars, where i is the inclination of the rotation axis. Rotation generates meridional circulation which cancels the diffusion in stellar plasma. Heavy metals with unaltered isotope mixture are pushed to the atmosphere from stellar interiors by radiative-driven diffusion (Michaud & Richer 2008), creating observed enhancement of mercury.

II group

Seven stars χ Lupi, ϕ Phe, 28 Her, HR 3302, AV Scl, 41 Eri A, and 46 Aql have highly predominant heaviest isotope ^{204}Hg. These stars are probably on the final stage of diffusive separation of isotopes, when lighter isotopes have settled down and overabundance of remaining isotope ^{204}Hg is determined by the usual radiative acceleration.

III group

The largest enigma is the phenomenon where two heaviest isotopes ^{204}Hg and ^{202}Hg are dominant in the atmosphere, as it is the case for 13 of the program stars. According to our results (Fig. 4.5) the expected isotopes during late evolutionary stages are ^{204}Hg and ^{201}Hg. Odd-A isotopes are additionally supported in the atmosphere due to hyperfine splitting of their lines. It is possible, that due to this effect odd-A isotopes are pushed up into high layers of the atmosphere out of the line-forming region, as suggested by Michaud et al. (1974), see Section 1.3.2. Weak stellar wind would strengthen this process. As a result, isotopes ^{202}Hg and ^{204}Hg would dominate in the line-forming region. In addition, the observed microturbulence (not exceeding 1 km s^{-1} in HgMn stars) changes essentially the picture of overlap rates of the isotopic spectral lines and therefore also modifies evolutionary scenarios of isotope separation. Also presence of weak entangled magnetic fields can alter the process of isotope separation.

Combination of LID mechanism and separation scenario by Michaud et al. (1974) may be involved in forming Hg isotopic mixture found in 11 Per by Woolf & Lambert (1999). The isotopic mixture shows large abundances of ^{199}Hg and ^{204}Hg with small or zero abundances for the other five: 0.4% ^{196}Hg, 7.5% ^{198}Hg, 23.4% ^{199}Hg, 2.5% ^{200}Hg, 0.8% ^{201}Hg, 1.2% ^{202}Hg, and 64.1% ^{204}Hg. Woolf & Lambert (1999) write: "There seems to be no way to use diffusion to explain

the bizarre Hg isotopic mix found in 11 Per. It may be possible to explain the missing ^{201}Hg in HR 7245 by hyperfine splitting, but 11 Per has low abundances of ^{200}Hg, ^{201}Hg, and ^{202}Hg, sandwiched between high abundances of ^{199}Hg and ^{204}Hg. Mass differences cannot be invoked to explain this isotopic mix. The even isotopes do not have hyperfine splitting to desaturate their lines and increase radiative acceleration. Diffusion fails as an explanation." However, deficiency of light even-A isotopes and overabundance of ^{204}Hg may be caused by LID, while ^{201}Hg may be wiped out of the atmosphere by high radiative pressure. High concentration of ^{199}Hg may be also explained by radiative pressure amplified by hyperfine splitting. Increase of $a^{\rm rad}$ for ^{199}Hg is not, however, as large as for ^{201}Hg. As a result, ^{199}Hg is effectively supported in the line-forming region of the atmosphere. Detailed model computations are certainly necessary to validate this scenario, but it seems that even such a bizarre isotopic mixture can be explained by diffusion, if LID is taken into account in addition to the usual radiative acceleration.

CHAPTER 5
DISCUSSION

The most important conclusion of the study is that the light-induced drift plays important role in triggering and generating diffusional separation of isotopes of heavy elements in the quiescent atmospheres of chemically peculiar stars. Our model computations also show that abundances of mercury isotopes vary throughout the stellar atmosphere. Observational evidence for such vertical abundance stratification in several types of stars has accumulated over recent years.

In mercury-rich atmospheres LID causes sinking of lighter isotopes and rising of heavier ones, leading to the separation of isotopes. Similar separation is expected also for isotopes of other heavy metals. On the contrary, for light elements like helium with opposite direction of isotopic shift of spectral lines, rising of lighter isotopes and sinking heavier ones is expected. The diffusion process is essentially more complicated if the hyperfine splitting of spectral lines of isotopes with odd number of nucleons is present. Non-trivial isotope anomalies are observed in many mercury-manganese CP star atmospheres, the genesis of which demands special additional studies.

Time-dependent models of diffusion in stellar atmospheres should be in future coupled with stellar evolution models, which take into account radiative-driven diffusion in stellar interiors. The first step would be to use concentrations at the bottom of atmosphere obtained with stellar evolution models as input to the atmospheric code. This approach is justified since diffusion processes in the atmosphere proceed essentially quicker than in the interiors.

To describe more realistically the CP star atmospheres also the microturbulence and weak stellar wind as diffusion decelerators and limiters should be taken into account. The microturbulence phenomenon is assumed to be related to helium or to plasma instabilities, but the adequate theory is still lacking. The influence of microturbulence on the diffusion can be expressed via an additional turbulent diffusion coefficient D_T added to the expression of the diffusion velocity (Schatzman 1969), namely

$$V_i = a_i t_i - (\Delta_i + D_T)\frac{d\ln\rho C_i}{dr}.$$

Study of spectral line profiles has shown that the characteristic velocity of microturbulence in chemically peculiar stars does not exceed the mean thermal velocity of heavy metals but the characteristic dimensions, especially the characteristic height of these turbulence eddies remain open and apparently require extensive additional studies. In any case, probably $D_T \gg \Delta_i$ holds and as a result, the dif-

fusive evolution may be several dex slower than in the case of an ideally quiescent stellar atmosphere. In addition to the deceleration of diffusion, turbulence should also lead to the essentially smaller equilibrium gradient of concentration C_i. Further analysis is necessary for proper treatment of influence of microturbulence on the diffusion processes in stellar plasma.

The peculiarities of radiative-driven diffusion in magnetic CP stars have not been studied here. The process in magnetic stellar atmospheres is essentially more complicated than in the non-magnetic ones. The first step would be to specify the configuration of the magnetic field and thereby take into account that diffusion of charged particles in the direction perpendicular to the magnetic field is heavily braked (Chapman & Cowling 1970; Vauclair et al. 1979; Hui-Bon-Hoa et al. 1996). The second physical process that modifies diffusion in magnetic stars is Zeeman effect (Alecian & Stift 2002, 2004). Alecian & Stift (2006, 2007, 2008) have elaborated an atmospheric code CARAT for modelling equilibrium element stratification due to atomic diffusion in magnetic stars.

CHAPTER 6
MAIN RESULTS OF THE THESIS

1. The formulae, describing light-induced drift in quiescent atmospheres of CP stars due to asymmetry of radiative flux in wings of overlapping isotopic spectral lines, have been derived. Effect of light-induced drift in stellar atmospheres can be reduced to the equivalent acceleration to be added to the usual radiative acceleration.

2. Adequate approximations have been found for cross-sections and transition rates of several quantum physical interaction processes involved into LID generation.

3. Computer code SMART, composed primarily for modelling of stellar atmospheres and stellar spectra, has been supplemented with additional software blocks for computation of evolutionary scenarios of diffusional separation of isotopes of chemical elements.

4. The data bank of splitted spectral lines of mercury has been composed. Both the isotopic and hyperfine splitting have been incorporated for adequate study of light-induced drift due to overlapping spectral line components of Hg isotopes.

5. Evolutionary scenarios of mercury isotope separation have been computed for solar, solar + 3 dex and solar + 5 dex initial mercury abundances with solar ratios of isotopes at effective temperatures 9 500 K, 10 750 K and 12 000 K. The main features of evolutionary separation of mercury isotopes have been elucidated.

6. Light-induced drift resulting from systematically blended isotopic lines causes diffusive separation of isotopes which may explain anomalous isotope ratios observed in the CP stellar atmospheres. Model computations confirm the important role of light-induced drift in the evolutionary separation of mercury isotopes in the quiescent atmospheres of chemically peculiar HgMn stars.

ACKNOWLEDGEMENTS

I am deeply grateful to my supervisor Arved Sapar for patient supervision and teaching during many years. I am also very thankful for his advices on improving my manuscript.

My sincere gratitude goes to my colleagues at the Tartu Observatory Lili Sapar and Raivo Poolamäe for the fruitful long-term collaboration and their contribution to the studies.

I would like to thank Indrek Martinson, Sveneric Johansson† and Glenn Wahlgren from Atomic Spectroscopy Group, Department of Physics, University of Lund for their support and hospitality during my stays at the Lund University in 1996 – 1997. This cooperation provided vital support to my research and also allowed an access to the computing facilities, which were not available at the Tartu Observatory at that time.

I am grateful to Swetlana Hubrig (European Southern Observatory), Tanya Ryabchikova (Institute of Astronomy of the Russian Academy of Sciences), Mike Dworetsky (University College London) and Francis LeBlanc (Université de Moncton, Canada) for inspiring discussions during several meetings.

I gratefully acknowledge the financial support by the Estonian Science Foundation (the grants held by Arved Sapar).

17

REFERENCES

Adelman, S. J. 1987, MNRAS, 228, 573

Adelman, S. J. 1988, MNRAS, 235, 749

Adelman, S. J. 1989, MNRAS, 239, 487

Adelman, S. J. 1992, MNRAS, 258, 167

Adelman, S. J. 1994, MNRAS, 266, 97

Adelman, S. J., Adelman, A. S., & Pintado, O. I. 2003, A&A, 397, 267

Adelman, S. J., Caliskan, H., Gulliver, A. F., & Teker, A. 2006, A&A, 447, 685

Adelman, S. J. & Cowley, C. R. 1986, in Astrophysics and Space Science Library, Vol. 125, IAU Colloq. 90: Upper Main Sequence Stars with Anomalous Abundances, ed. C. R. Cowley, M. M. Dworetsky, & C. Megessier, 305–313

Adelman, S. J., Gulliver, A. F., & Rayle, K. E. 2001, A&A, 367, 597

Adelman, S. J., Proffitt, C. R., Wahlgren, G. M., Leckrone, D. S., & Dolk, L. 2004, ApJS, 155, 179

Alecian, G. & Stift, M. J. 2002, A&A, 387, 271

Alecian, G. & Stift, M. J. 2004, A&A, 416, 703

Alecian, G. & Stift, M. J. 2006, A&A, 454, 571

Alecian, G. & Stift, M. J. 2007, A&A, 475, 659

Alecian, G. & Stift, M. J. 2008, Contributions of the Astronomical Observatory Skalnate Pleso, 38, 113

Anders, E. & Grevesse, N. 1989, Geochim. Cosmochim. Acta, 53, 197

Aret, A. & Sapar, A. 2002, Astronomische Nachrichten, 323, 21

Aret, A., Sapar, A., Poolamäe, R., & Sapar, L. 2008, in IAU Symposium, Vol. 252, The Art of Modeling Stars in the 21st Century, ed. L. Deng & K.-L. Chan (Cambridge University Press), 41–42

Asplund, M., Grevesse, N., & Sauval, A. J. 2005, in Astronomical Society of the Pacific Conference Series, Vol. 336, Cosmic Abundances as Records of Stellar Evolution and Nucleosynthesis, ed. T. G. Barnes, III & F. N. Bash, 25–+

Atutov, S. N. 1986, Physics Letters A, 119, 121

Atutov, S. N., Lesjak, S., Podjachev, S. P., & Shalagin, A. M. 1986, Optics Communications, 60, 41

Atutov, S. N. & Shalagin, A. M. 1988, Soviet Astronomy Letters, 14, 284

Baron, E. & Hauschildt, P. H. 1998, ApJ, 495, 370

Bidelman, W. P. 1962, AJ, 67, 111

Bidelman, W. P. 1967, in Magnetic and Related Stars, ed. R. C. Cameron, 29–+

Bohlender, D. 2005, in EAS Publications Series, Vol. 17, EAS Publications Series, ed. G. Alecian, O. Richard, & S. Vauclair, 83–88

Bohlender, D. A., Dworetsky, M. M., & Jomaron, C. M. 1998, ApJ, 504, 533

Borra, E. F. & Landstreet, J. D. 1980, ApJS, 42, 421

Brandt, J. C., Heap, S. R., Beaver, E. A., et al. 1999, AJ, 117, 1505, pDF available

Bransden, B. H. & Joachain, C. J. 2003, Physics of Atoms and Molecules, 2nd edn. (Prentice Hall)

Burgers, J. M. 1969, Flow Equations for Composite Gases (New York: Academic Press)

Cannon, A. J. 1912a, Annals of Harvard College Observatory, 56, 113

Cannon, A. J. 1912b, Annals of Harvard College Observatory, 56, 161

Castelli, F. & Hubrig, S. 2004a, A&A, 425, 263

Castelli, F. & Hubrig, S. 2004b, A&A, 421, L1

Castelli, F. & Hubrig, S. 2007, A&A, 475, 1041

Cayrel, R., Burkhart, C., & van't Veer, C. 1991, in IAU Symposium, Vol. 145, Evolution of Stars: the Photospheric Abundance Connection, ed. G. Michaud & A. V. Tutukov, 99–+

Chapman, S. & Cowling, T. G. 1970, The mathematical theory of non-uniform gases. An account of the kinetic theory of viscosity, thermal conduction and diffusion in gases, 3rd edn. (Cambridge: University Press)

Conti, P. S. 1969, ApJ, 156, 661

Cowley, C. R. & Aikman, G. C. L. 1975, PASP, 87, 513

Cowley, C. R. & Bord, D. J. 2004, in IAU Symposium, Vol. 224, The A-Star Puzzle, ed. J. Zverko, J. Ziznovsky, S. J. Adelman, & W. W. Weiss, 265–281

Cowley, C. R. & Day, C. A. 1976, ApJ, 205, 440

Cowley, C. R. & Hubrig, S. 2005, A&A, 432, L21

Cowley, C. R., Hubrig, S., & Castelli, F. 2008, Contributions of the Astronomical Observatory Skalnate Pleso, 38, 291

Cowley, C. R., Hubrig, S., Castelli, F., González, J. F., & Wolff, B. 2007, MNRAS, 377, 1579

Cowley, C. R., Hubrig, S., & Gonzalez, F. G. 2009, e-print arXiv:0903.0611

Cowley, C. R., Hubrig, S., González, G. F., & Nuñez, N. 2006, A&A, 455, L21

Dolk, L., Wahlgren, G. M., & Hubrig, S. 2003, A&A, 402, 299

Dworetsky, M. M. & Vaughan, Jr., A. H. 1973, ApJ, 181, 811

Eddington, A. S. 1926, The Internal Constitution of the Stars (The Internal Constitution of the Stars, Cambridge: Cambridge University Press, 1926)

Fowler, W. A., Burbidge, E. M., Burbidge, G. R., & Hoyle, F. 1965, ApJ, 142, 423

Gel'mukhanov, F. K. & Shalagin, A. M. 1979, Soviet Journal of Experimental and Theoretical Physics Letters, 29, 711

Gonzalez, J.-F., LeBlanc, F., Artru, M.-C., & Michaud, G. 1995, A&A, 297, 223

Griem, H. R., Kolb, A. C., & Shen, K. Y. 1959, Physical Review, 116, 4

Guthrie, B. N. G. 1967, Publications of the Royal Observatory of Edinburgh, 6, 145

Hartoog, M. R. & Cowley, A. P. 1979, ApJ, 228, 229

Hauschildt, P. H., Allard, F., & Baron, E. 1999, ApJ, 512, 377

Hauschildt, P. H. & Baron, E. 1999, Journal of Computational and Applied Mathematics, 109, 41

Hauschildt, P. H., Baron, E., & Allard, F. 1997, ApJ, 483, 390

Havnes, O. & Conti, P. S. 1971, A&A, 14, 1

Heacox, W. D. 1979, ApJS, 41, 675

Heber, U. 1991, in IAU Symposium, Vol. 145, Evolution of Stars: the Photospheric Abundance Connection, ed. G. Michaud & A. V. Tutukov, 363–+

Herbig, G. H. 1965, ApJ, 141, 588

Hill, G. M. & Landstreet, J. D. 1993, A&A, 276, 142

Hubrig, S. & Castelli, F. 2001, A&A, 375, 963, pDF available

Hubrig, S., Castelli, F., & Mathys, G. 1999, A&A, 341, 190

Hubrig, S., North, P., Schöller, M., & Mathys, G. 2006, Astronomische Nachrichten, 327, 289

Hui-Bon-Hoa, A., Alecian, G., & Artru, M.-C. 1996, A&A, 313, 624

Hui-Bon-Hoa, A., LeBlanc, F., & Hauschildt, P. H. 2000, ApJ, 535, L43

Humlíček, J. 1979, J. Quant. Spec. Radiat. Transf., 21, 309

Johansson, S., Kalus, G., Brage, T., Leckrone, D. S., & Wahlgren, G. M. 1996, ApJ, 462, 943

Jomaron, C. M., Dworetsky, M. M., & Bohlender, D. A. 1998, Contributions of the Astronomical Observatory Skalnaté Pleso, 27, 324

Kalus, G., Johansson, S., Wahlgren, G. M., et al. 1998, ApJ, 494, 792

Khalack, V. R., Leblanc, F., Behr, B. B., Wade, G. A., & Bohlender, D. 2008, A&A, 477, 641

Khalack, V. R., Leblanc, F., Bohlender, D., Wade, G. A., & Behr, B. B. 2007, A&A, 466, 667

Kupka, F. G., Ryabchikova, T. A., Piskunov, N. E., Stempels, H. C., & Weiss, W. W. 2000, Baltic Astronomy, 9, 590

Kurtz, D. W., Freyhammer, L. M., Elkin, V. G., & Mathys, G. 2007, in American Institute of Physics Conference Series, Vol. 948, Unsolved Problems in Stellar Physics: A Conference in Honor of Douglas Gough, ed. R. J. Stancliffe, G. Houdek, R. G. Martin, & C. A. Tout, 249–256

Kurucz, R. 1993a, ATLAS9 Stellar Atmosphere Programs and 2 km/s grid. Kurucz CD-ROM No. 13. Cambridge, Mass.: Smithsonian Astrophysical Observatory, 1993., 13

Kurucz, R. 1993b, SYNTHE Spectrum Synthesis Programs and Line Data. Kurucz CD-ROM No. 18. Cambridge, Mass.: Smithsonian Astrophysical Observatory, 1993., 18

Kurucz, R. & Bell, B. 1995, Atomic Line Data (R.L. Kurucz and B. Bell) Kurucz CD-ROM No. 23. Cambridge, Mass.: Smithsonian Astrophysical Observatory, 1995., 23

Landstreet, J. D. 1982, ApJ, 258, 639

Lanz, T. 1993, in ASP Conf. Ser. 44: IAU Colloq. 138: Peculiar versus Normal Phenomena in A-type and Related Stars, 60–+

LeBlanc, F. & Michaud, G. 1993, ApJ, 408, 251

Leblanc, F. & Monin, D. 2004, in IAU Symposium, Vol. 224, The A-Star Puzzle, ed. J. Zverko, J. Ziznovsky, S. J. Adelman, & W. W. Weiss, 193–200

Leblanc, F., Monin, D., Hui-Bon-Hoa, A., & Hauschildt, P. H. 2009, A&A, 495, 937

Leckrone, D. S. 1984, ApJ, 286, 725

Leckrone, D. S., Johansson, S., Kalus, G., et al. 1996, ApJ, 462, 937

Leckrone, D. S., Proffitt, C. R., Wahlgren, G. M., Johansson, S. G., & Brage, T. 1999, AJ, 117, 1454, pDF available

Masana, E., Jordi, C., Maitzen, H. M., & Torra, J. 1998, A&AS, 128, 265

Mathys, G. & Hubrig, S. 1995, A&A, 293, 810

Michaud, G. 1970, ApJ, 160, 641

Michaud, G., Charland, Y., Vauclair, S., & Vauclair, G. 1976, ApJ, 210, 447

Michaud, G., Reeves, H., & Charland, Y. 1974, A&A, 37, 313

Michaud, G. & Richer, J. 2008, Contributions of the Astronomical Observatory Skalnate Pleso, 38, 103

Michaud, G., Richer, J., & Richard, O. 2005, ApJ, 623, 442

Michaud, G., Richer, J., & Richard, O. 2007, ApJ, 670, 1178

Michaud, G., Richer, J., & Richard, O. 2008, ApJ, 675, 1223

Michaud, G., Tarasick, D., Charland, Y., & Pelletier, C. 1983, ApJ, 269, 239

Milne, E. A. 1927, MNRAS, 87, 697

Nasyrov, K. A. & Shalagin, A. M. 1993, A&A, 268, 201

North, P. 1993, in Astronomical Society of the Pacific Conference Series, Vol. 44, IAU Colloq. 138: Peculiar versus Normal Phenomena in A-type and Related Stars, ed. M. M. Dworetsky, F. Castelli, & R. Faraggiana, 577–+

Paquette, C., Pelletier, C., Fontaine, G., & Michaud, G. 1986, ApJS, 61, 177

Polosukhina, N., Shavrina, A., Drake, N. A., et al. 2004, in IAU Symposium, Vol. 224, The A-Star Puzzle, ed. J. Zverko, J. Ziznovsky, S. J. Adelman, & W. W. Weiss, 665–672

Polosukhina, N. S. & Shavrina, A. V. 2007, Astrophysics, 50, 381

Popov, A. K., Shalagin, A. M., Streater, A. D., & Woerdman, J. P. 1989, Phys. Rev. A, 40, 867

Praderie, F. 2005, in EAS Publications Series, Vol. 17, EAS Publications Series, ed. G. Alecian, O. Richard, & S. Vauclair, 3–8

Preston, G. 2005, in EAS Publications Series, Vol. 17, EAS Publications Series, ed. G. Alecian, O. Richard, & S. Vauclair, 9–14

Preston, G. W. 1974, ARA&A, 12, 257

Proffitt, C. R., Brage, T., & Leckrone, D. S. 1996, in Astronomical Society of the Pacific Conference Series, Vol. 108, M.A.S.S., Model Atmospheres and Spectrum Synthesis, ed. S. J. Adelman, F. Kupka, & W. W. Weiss, 103–+

Proffitt, C. R., Brage, T., Leckrone, D. S., et al. 1999, ApJ, 512, 942

Richard, O., Michaud, G., & Richer, J. 2002a, ApJ, 580, 1100

Richard, O., Michaud, G., Richer, J., et al. 2002b, ApJ, 568, 979

Richer, J., Michaud, G., & Turcotte, S. 2000, ApJ, 529, 338

Romanyuk, I. I. 2007, Astrophysical Bulletin, 62, 62

Rosman, K. J. R. & Taylor, P. D. P. 1998, Journal of Physical and Chemical Reference Data, 27, 1275

Ryabchikova, T. 2008, Contributions of the Astronomical Observatory Skalnate Pleso, 38, 257

Ryabchikova, T., Kochukhov, O., & Bagnulo, S. 2007, in Physics of Magnetic Stars, 325–334

Ryabchikova, T., Kochukhov, O., & Bagnulo, S. 2008, A&A, 480, 811

Ryabchikova, T. A. 1991, in IAU Symposium, Vol. 145, Evolution of Stars: the Photospheric Abundance Connection, ed. G. Michaud & A. V. Tutukov, 149–+

Sapar, A. & Aret, A. 1995, Astronomical and Astrophysical Transactions, 7, 1

Sapar, A., Aret, A., & Poolamäe, R. 2005, in EAS Publications Series, Vol. 17, Element Stratification in Stars: 40 Years of Atomic Diffusion, ed. G. Alecian, O. Richard, & S. Vauclair, 341–344

Sapar, A., Aret, A., Sapar, L., & Poolamäe, R. 2007a, in Spectroscopic Methods in Modern Astrophysics, ed. L. Mashonkina & M. Sachkov (Moscow: Janus-K), 220–235

Sapar, A., Aret, A., Sapar, L., & Poolamäe, R. 2008a, in ESO Astrophysics Symposia, Vol. 22, Precision Spectroscopy in Astrophysics. Proceedings of the ESO/Lisbon/Aveiro Workshop, Lisborn/Aveiro, Portugal, 11–15 September 2006, ed. N. C. Santos, L. Pasquini, A. C. M. Correia, & M. Romaniello, 145–148

Sapar, A., Aret, A., Sapar, L., & Poolamäe, R. 2008b, Contributions of the Astronomical Observatory Skalnaté Pleso, 38, 445

Sapar, A. & Poolamäe, R. 2003, in Astronomical Society of the Pacific Conference Series, Vol. 288, Stellar Atmosphere Modeling, ed. I. Hubeny, D. Mihalas, & K. Werner, 95–+

Sapar, A., Poolamäe, R., Sapar, L., & Aret, A. 2007b, in Spectroscopic Methods in Modern Astrophysics, ed. L. Mashonkina & M. Sachkov (Moscow: Janus-K), 236–254

Sargent, A. W. L. W. & Jugaku, J. 1961, ApJ, 134, 777

Savanov, I. & Hubrig, S. 2003, A&A, 410, 299

Schatzman, E. 1969, A&A, 3, 331

Schneider, H. 1986, in Astrophysics and Space Science Library, Vol. 125, IAU Colloq. 90: Upper Main Sequence Stars with Anomalous Abundances, ed. C. R. Cowley, M. M. Dworetsky, & C. Megessier, 205–208

Shulyak, D., Kochukhov, O., & Khan, S. 2008, A&A, 487, 689

Shulyak, D., Tsymbal, V., Ryabchikova, T., Stütz, C., & Weiss, W. W. 2004, A&A, 428, 993

Smith, K. C. 1993, A&A, 276, 393

Smith, K. C. 1994, A&A, 291, 521

Smith, K. C. 1996a, Ap&SS, 237, 77

Smith, K. C. 1996b, A&A, 305, 902

Smith, K. C. 1997, A&A, 319, 928

Smith, K. C. & Dworetsky, M. M. 1993, A&A, 274, 335

Striganov, A. R. & Dontsov, Y. P. 1955, Uspekhi Fizicheskikh Nauk, 55, 315

Takada-Hidai, M. 1991, in IAU Symposium, Vol. 145, Evolution of Stars: the Photospheric Abundance Connection, ed. G. Michaud & A. V. Tutukov, 137–+

Thiam, M., Wade, G. A., Leblanc, F., & Khalack, V. R. 2008, Contributions of the Astronomical Observatory Skalnate Pleso, 38, 461

Thoul, A. & Montalbán, J. 2007, in EAS Publications Series, Vol. 26, Stellar Evolution and Seismic Tools for Asteroseismology – Diffusive Processes in Stars and Seismic Analysis, ed. C. W. Straka, Y. Lebreton, & M. J. P. F. G. Monteiro, 25–36

Turcotte, S. & Richard, O. 2005, in EAS Publications Series, Vol. 17, EAS Publications Series, ed. G. Alecian, O. Richard, & S. Vauclair, 357–360

VandenBerg, D. A., Richard, O., Michaud, G., & Richer, J. 2002, ApJ, 571, 487

Vauclair, G., Vauclair, S., & Michaud, G. 1978, ApJ, 223, 920

Vauclair, S. 2005, in EAS Publications Series, Vol. 17, EAS Publications Series, ed. G. Alecian, O. Richard, & S. Vauclair, 119–131

Vauclair, S., Hardorp, J., & Peterson, D. M. 1979, ApJ, 227, 526

Vauclair, S. & Vauclair, G. 1982, ARA&A, 20, 37

Wahlgren, G. M. & Dolk, L. 1998, Contributions of the Astronomical Observatory Skalnate Pleso, 27, 314

Wahlgren, G. M., Dolk, L., Kalus, G., et al. 2000, ApJ, 539, 908

Wahlgren, G. M., Leckrone, D. S., Brage, T., Proffitt, C. R., & Johansson, S. 1998, in Astronomical Society of the Pacific Conference Series, Vol. 143, The Scientific Impact of the Goddard High Resolution Spectrograph, ed. J. C. Brandt, T. B. Ake, & C. C. Petersen, 330–+

Wahlgren, G. M., Leckrone, D. S., Johansson, S. G., Rosberg, M., & Brage, T. 1995, ApJ, 444, 438

Werner, K. & Dreizler, S. 1999, Journal of Computational and Applied Mathematics, 109, 65

White, R. E., Vaughan, Jr., A. H., Preston, G. W., & Swings, J. P. 1976, ApJ, 204, 131

Wolff, S. C. 1983, The A-stars: Problems and perspectives. Monograph series on nonthermal phenomena in stellar atmospheres (The A-stars: Problems and perspectives. Monograph series on nonthermal phenomena in stellar atmospheres)

Wolff, S. C. & Preston, G. W. 1978, ApJS, 37, 371

Woolf, V. M. & Lambert, D. L. 1999, ApJ, 521, 414, available as pdf

Zakharova, L. A. & Ryabchikova, T. A. 1996, Astronomy Letters, 22, 152

SUMMARY IN ESTONIAN

Elavhõbeda isotoopide lahknemiskulg keemiliselt pekuliaarsete tähtede atmosfäärides

Keemiliselt pekuliaarsed (CP) tähed on kuumad peajada tähed paljude keemiliste elementide ebatavalise sisaldusega. Üldlevinud arvamuse kohaselt tekivad need anomaalsed sisaldused täheatmosfääris, samas kui kogu tähe keemiline koostis jääb tavaliseks. Umbes 40 aastat tagasi pakkus G. Michaud (1970) välja idee, et anomaalne keemiline koostis tekib täheatmosfäärides kiirguse poolt kujundatava atomaardifusiooni tagajärjel. Aeglane difusiooniprotsess pääseb mõjule ainult rahulikes täheatmosfäärides, kus makroliikumised on nõrgad. Peajada tähtede puhul on see tingimus täidetud efektiivsete temperatuuride vahemikus 7 000 kuni 20 000 K. Kuigi CP tähtede tekkimise kohta on esitatud mitmeid hüpoteese, suudab vaid difusiooniteooria pakkuda rahuldavat seletust mitmekesistele keemiliste elementide sisalduse anomaaliatele. Siiski tekib difusiooniteooria rakendamisel olulisi raskusi isotoopkoostise anomaaliate seletamisega. Ka mõningate elementide ülisuurte liiasuste tekkimiseks ei piisa vaid kiirgusrõhu mõjust.

S. Atutov ja A. Shalagin (1988) jõudsid järeldusele, et laboritingimustes avastatud ja uuritud valgusindutseeritud triivi (LID) efekt võib põhjustada CP tähtedes vaadeldavaid sisaldusanomaaliaid. Valgusindutseeritud triivi efekt tekib siis, kui soojusliikumises olevad aatomid ja ioonid neelavad kiirgust asümmetrilise profiiliga spektrijoones. Sellise kiirgusvoo neelamisel ergastatakse erinev arv täheatmosfääris üles- ja allapoole liikuvaid osakesi. Kuna atomaarosakeste põrkeristlõiked suurenevad nende ergastamisel ja osakeste liikuvus seetõttu väheneb, siis tekib osakeste liikuvuse asümmeetria, mis viibki LIDi tekkimisele.

Sõltuvalt kiirgusvoo asümmeetria kujust spektrijoones võib kujuneda triiv, mis on suunatud täheatmosfääris kas üles- või allapoole. Reeglina on spektrijoonte asümmeetria juhuslik, mistõttu on juhuslik ka erinevates spektrijoontes tekkiva triivikiiruse suund ja suurus. Tulemusena on summaarne valgusindutseeritud triiv võrreldes tavalise kiirguskiirendusega ebaoluline. Isotoopide puhul aga tekib süstemaatiline spektrijoonte profiilide asümmeetria, kuna nende omavahel nihkes, kuid osaliselt kattuvad spektrijooned põhjustavad kõikides spektrijoontes sarnase kujuga asümmeetria. Näiteks elavhõbeda (ja ka teiste raskete elementide) kergeima isotoobi spektrijoonte punane tiib on alati blendeeritud raskemate isotoopide poolt, raskeima isotoobi spektrijoontes on aga blendeeritud sinine tiib. Seega summaarne LID on kergeima isotoobi puhul suunatud täheatmosfääris allapoole, raskeima isotoobi puhul aga ülespoole. Valgusindutseeritud triivi rolli selgitamine elavhõbeda isotoopide difusioonilisel lahknemisel CP tähtede atmosfäärides ongi käesoleva väitekirja peaeesmärk.

On tuletatud analüütilised valemid, mis kirjeldavad valgusindutseeritud triivi CP tähtede atmosfääridele vastavates füüsikalistes tingimustes. LIDi mõju saab taandada ekvivalentseks kiirenduseks, mis tuleb lisada tavalisele kiirguskiirendusele. On leitud sobivad lähendid mitmete LIDi mõjutavate põrkeprotsesside ristlõigete ja tõenäosuste arvutamiseks.

Programmi SMART, mis on koostatud kuumade tähtede mudelatmosfääride ja spektrite arvutamiseks ning mitmesuguste neis toimuvate füüsikaliste protsesside uurimiseks, on täiendatud programmiblokkidega, mis võimaldavad modelleerida isotoopide lahknemiskulgu raskusjõu, kiirgusrõhu ja LIDi koosmõjul.

Elavhõbeda isotoopide lahknemise modelleerimiseks on koostatud spektrijoonte nimekiri, mis sisaldab umbes 700 Hg I, Hg II ja Hg III iooni resonants- ja subordinaatjoont. On arvestatud nii joonte isotoop- kui ka ülipeenstruktuurset lõhenemist, mis on olulised valgusindutseeritud triivi arvutamiseks.

Elavhõbeda isotoopide lahknemiskulgu on arvutatud mudelatmosfääride valimi jaoks kolmel efektiivsel temperatuuril ($T_{\rm eff}$ = 9 500 K, 10 750 K, 12 000 K) ja kolme elavhõbeda algsisaldusega (ρ^0 = päikese, päikese + 3 suurusjärku ja päikese + 5 suurusjärku sisaldusega). Kõikide mudelatmosfääride puhul eeldati, et $\log g = 4, V_{\rm rot} = 0, V_{\rm turb} = 0$. Modelleerimise alghetkel loeti elavhõbeda sisaldus ühtlaseks kogu atmosfääris ja vastavaks päikesesüsteemi isotoopkoostisele. Võimalikku tähetuule ja mikroturbulentsi olemasolu, mis pidurdaksid difusiooni, ei arvestatud. Valgusindutseeritud triivi arvutamine nõuab ülitäpseid spektraalandmeid ja kõrge lahutusega (kuni $\lambda/\Delta\lambda = 5\ 000\ 000$) sünteetilise spektri arvutamist kõigis atmosfääri kihtides. Kuna atmosfääri väliskihtides on osakeste vaba tee oluliselt pikem kui sügavates kihtides, toimub difusioon seal ka oluliselt kiiremini. Mitmeid suurusjärke erinevad karakteersed lahknemisajad põhjustavad olulisi arvutusraskusi, mille ületamiseks on nähtud palju vaeva.

Töö põhitulemuseks on valgusindutseeritud triivi olulise rolli kindlakstegemine isotoopide separeerumisel CP tähtede atmosfäärides. Mudelarvutuste tulemusena selgus ka vertikaalsete sisaldusprofiilide kujunemine täheatmosfääris, mida kinnitavad ka viimasel ajal kogutud vaatlusandmed. Elavhõbedarikastes HgMn tähede atmosfäärides põhjustab LID järjestikust kergemate isotoopide vajumist ja raskemate isotoopide kerkimist. Samalaadset efekti võib oodata ka teiste raskmetallide puhul. Spektrijoonte ülipeenstruktuurse lõhenemise arvestamine teeb lahknemisprotsessi oluliselt keerulisemaks, kuna paaritute isotoopide spektrijoonte ülipeenstruktuursed komponendid asuvad isotoopjoonte suhtes ebakorrapäraselt.

HgMn tähtede fenomen on mitme füüsikalise protsessi koosmõju tulemus. Lisaks difusioonile tuleks arvestada ka mikroturbulentsi, tähetuule ja (nõrkade) magnetväljade mõju. Täheevolutsioonist ja -kaksiklusest tulenevad nähtused võivad samuti mõjutada anomaaliate kujunemise kulgu CP tähtedes.

CURRICULUM VITAE

Name:	Anna Aret
Date and place of birth:	December 22, 1964, Voronezh, Russia
Citizenship:	Estonian
Current employment:	Tartu Observatory (research associate)
Address:	Tartu Observatory 61602 Tõravere Tartumaa, Estonia
Phone:	(+372) 741 0465
Fax:	(+372) 741 0205
E-mail:	aret@aai.ee

Education:

The 1st Secondary School of Kemerovo, Russia, 1982
Moscow State University, diploma in physics (*cum laude*), 1989
University of Tartu, MSc in physics, 1993

Research and professional experience:

1989 – 1992:	Institute of Astrophysics and Atmospheric Physics, junior research associate
1993 – 1998:	University of Tartu, PhD student
1995 – ...	Tartu Observatory, research associate
1996 – 1997:	Lund University, researcher

Field of research:

Theoretical astrophysics: processes in stellar atmospheres and stellar winds, processing and study of stellar spectra

ELULUGU

Nimi:	Anna Aret
Sünniaeg ja koht:	22. detsember 1964, Voronež, Venemaa
Kodakondsus:	Eesti
Praegune töökoht (amet):	Tartu Observatoorium (teadur)
Aadress:	Tartu Observatoorium
	61602 Tõravere, Tartumaa
Telefon:	(+372) 741 0465
Faks:	(+372) 741 0205
E-post:	aret@aai.ee

Haridus:

Kemerovo I Keskkool, Venemaa, 1982
Moskva Riiklik Ülikool, füüsika (*cum laude*), 1989
Tartu Ülikool, magistrikraad (teaduskraad) füüsika alal, 1993

Teenistuskäik:

1989 – 1992:	Astrofüüsika ja Atmosfäärifüüsika Instituut, nooremteadur
1993 – 1998:	Tartu Ülikool, doktorant
1995 – ...	Tartu Observatoorium, teadur
1996 – 1997:	Lundi Ülikool, teadur

Teadustöö põhisuunad:

Teoreetiline astrofüüsika: täheatmosfääride ja tähetuule füüsika, tähespektrite töötlus ja uurimine

DISSERTATIONES ASTRONOMIAE UNIVERSITATIS TARTUENSIS

1. **Tõnu Viik.** Numerical realizations of analytical methods in theory of radiative transfer. Tartu, 1991.
2. **Enn Saar.** Geometry of the large scale structure of the Universe. Tartu, 1991.
3. **Maret Einasto.** Morphological and luminosity segregation of galaxies. Tartu, 1991.
4. **Urmas Haud.** Dark Matter in galaxies. Tartu, 1991.
5. **Eugene A. Ustinov.** Inverse problems of radiative transfer in sounding of planetary atmospheres. Tartu, 1992.
6. **Peeter Tenjes.** Models of regular galaxies. Tartu, 1993.
7. **Ivar Suisalu.** Simulation of the evolution of large scale structure elements with adaptive multigrid method. Tartu, 1995.
8. **Teimuraz Shvelidze.** Automated quantitative spectral classification of stars by means of objective prism spectra: the method and applications. Tartu, 1999.
9. **Jelena Gerškevitš.** Formation and evolution of binary systems with compact objects. Tartu, 2002.
10. **Ivan Suhhonenko**. Large-scale motions in the universe. Tartu, 2003.
11. **Antti Tamm.** Structure of distant disk galaxies. Tartu, 2006.
12. **Vladislav-Veniamin Pustynski.** Modeling the reflection effect in pre-cataclysmic binary systems. Tartu, 2007.